Identification of typical eco-hydrological behaviours using InSAR allows landscape-scale mapping of peatland condition

Andrew V. Bradley[1], Roxane Andersen[2], Chris Marshall[2], Andrew Sowter[3], David J. Large[4]

[1]Department of Chemical and Environmental Engineering, Faculty of Engineering, Nottingham Geospatial Institute, Innovation Park, Jubilee Campus, Nottingham, NG7 2TU, UK
[2]Environmental Research Institute, University of Highlands and Islands, Castle Street, Thurso, Scotland, KW14 7JD, UK
[3]Terra Motion Limited, Ingenuity Centre, Innovation Park, Jubilee Campus, University of Nottingham, Nottingham. NG7 2TU, UK
[4]Department of Chemical and Environmental Engineering, Faculty of Engineering, University of Nottingham, Nottingham. NG7 2RG, UK

Correspondence to: Andrew V. Bradley (andrew.bradley1@nottingham.ac.uk)

Abstract. Better tools for rapid and reliable assessment of global peatland extent and condition are urgently needed to support action to prevent their further decline. Peatland surface motion is a response to changes in the water and gas content of a peat body regulated by the ecology and hydrology of a peatland system. Surface motion is therefore a sensitive measure of ecohydrological condition but has traditionally been impossible to measure at the landscape scale. Here we examine the potential of surface motion metrics derived from InSAR satellite radar to map peatland condition in a blanket bog landscape. We show that the timing of maximum seasonal swelling of the peat is characterized by a bimodal distribution. The first maximum usually in autumn is typical of 'stiffer' peat associated with steeper topographic gradients, peatland margins, degraded peatland and more often associated with 'shrub'- dominated vegetation communities. The second maximum usually in winter is typically associated with 'softer' peat typically found in low topographic gradients often featuring pool systems, and *Sphagnum* dominated vegetation communities. Specific conditions ~~associated with 'Sphagnum'~~of 'soft' and '~~shrub' communities~~stiff' peats are also determined by the amplitude of swelling and multi-annual average ~~multiannual~~ motion. Peatland restoration currently follows a re-wetting strategy~~,~~; however, our approach highlights that landscape setting appears to determine the optimal endpoint for restoration. Aligning expectation for restoration outcomes with landscape setting might optimise peatland stability and carbon storage. Importantly, deployment of this approach, based on surface motion dynamics, could support peatland mapping and management on a global scale.

1. Introduction

The conservation of ~~functional~~well-functioning peatlands and ~~the~~ restoration of degraded ~~peatland~~peatlands, to reduce and ultimately mitigate land-use related emissions of atmospheric carbon dioxide, is now a global priority (Leifeld and Menichetti, 2018; Amelung et al., 2020; Günther et al., 2020). ~~To~~Furthermore, to support the implementation of national peatland management plans and restoration initiatives, cost-effective measures ~~of~~to record current peatland condition and restoration

Formatted Table

Formatted: Font: Italic

progress are urgently required (Crump, 2017). Mapping peatland extent and condition has long been recognized as a huge challenge over large, remote, wet, and often discontinuous peat forming regions where field-based surveys are impractical and expensive (Lees et al., 2018). Alternatives such as thematic mapping based on optical remote-sensing (visible and near-infra red) are increasingly used (Artz et al., 2018; Minasny et al., 2019; Lees et al., 2020), but the number of observations in regions with frequent cloud cover such as ~~peatlands~~peatland in the northern latitudes and the tropics reduces the number of possible surface observations. Radio detection and ranging (Radar) that is sensitive to physical properties of the surface, provides an effective, more frequent option, given that microwave frequencies can penetrate cloud cover and return a measured signal from the ground (Minasny et al., 2019; Poggio et al., 2014). For example, using the ESA Sentinel-1 Synthetic Aperture Radar (SAR) satellites it is now possible to observe a peatland surface anywhere at high frequency (6 to 12 days) with continuous spatial coverage. When this is combined with the technique of SAR Interferometry (InSAR) it allows detection of surface displacement, an indication of peatland condition, as a time-series of observations (Sowter et al., 2013).

In ~~peatlands~~peatland, the rise and fall of the surface, sometimes described as 'bog-breathing' (Kulczynski, 1949; Baden and Eggelsmann, 1964; Mustonon and Suena, 1971; Hutchinson, 1980; Kurimo, 1983; Almendinger et al., 1986; Price, 2003; Price and Schlotzhauer, 2003~~)~~), is one of the key self-regulating feedback mechanisms in peatland, providing resilience and maintaining function during periods of hydrological stress (Money and Wheeler, 1999; Waddington et al., 2015~~).~~; Mahdiyasa et al., 2021). This 'surface motion', which is a poro-elastic mechanical response to ecohydrological processes, results from the collapse and expansion of large pores in response to changes in the mass of water stored and associated stresses within the peat (Price, 2003~~).~~; Mahdiyasa et al., 2021). Mechanical deformation of the peat body and consequent surface motion can also modify the ecohydrology of a peatland via compaction, slope failure and pipe formation (Waddington et al., 2010; Waddington et al., 2015). Small-scale field observations indicate that peat surface motion is influenced by changes in water level (Roulet, 1991; Price, 2003; Kennedy and Price, 2005; Fritz at al., 2008; Alshammari et al., 2020), vegetation composition (Howie and Hebda, 2018; Alshammari et al., 2020), micro-topography (Waddington et al., 2010), accumulation and upward migration of methane bubbles (Glaser, et al., 2004; Reeve et al., 2013) and land management (Kennedy and Price, 2005).

Collectively these results suggest that peatland surface motion could be a sensitive indicator of peatland function on a landscape scale. So far, InSAR investigations have focused on discrete, small-scale (<1 km^2) peatlands (Fiaschi et al., 2019; Tampuu et al., 2020), identifying the potential range in timing and amplitude of seasonal peatland surface motion (Alshammari et al., ~~2020~~2018; Alshammari et al., ~~2018~~2020) and its relationship to precipitation (Fiaschi et al., 2019~~)~~), water level (Alshammari et al., 2020; Tampuu et al., 2020) and vegetation composition (Alshammari et al., 2020). However, peatland landscapes contain a continuum of topographic, ecological, hydrological and management regimes and these small-scale studies have not captured the full spectrum of peatland conditions between degraded and near natural.

In this paper, we determine whether surface motion measured by InSAR can be used to quantify ~~continuous changes in~~ peatland condition continuously over a complex peatland landscape. Using the APSIS (Advanced Pixel System using Intermittent ~~SBAS) InSAR method~~Small Baseline Subset, formerly known as the Intermittent Small Baseline Subset (ISBAS ~~(Sowter et~~

Formatted Table

al., 2013) (Materials and Methods))) method, which is capable of generating spatially continuous measures of vertical surface motion over peatland (Sowter et al., 2013)), we measure time series of surface motion over our study site at a high spatial and temporal resolution. Specific time series metrics are then compared to independent measures of peatland condition to determine their relationship. By doing this we relate surface motion metrics to the continuum of ecohydrological conditions in this peatland landscape. Finally, we demonstrate how surface motion metrics can be used to map the ecohydrology of a peatland system. By doing so we illustrate how our new approach could be applied to monitoring the response of global peatlandspeatland to restoration, management, and climate change.

2. Study Location

The Flow Country peatlands, Northern Scotland (Andersen et al., 2018) exist in a range of topographic, hydrological and management settings, leading to a range of different conditions e.g., highly eroded uplands to relatively intact low-lying peatland with pool systems, superimposed by activities such as forestry, drainage, and grazing. Our chosen study site is 930 km^2 of undulating blanket bog, ranging from 50 to 600 m.a.s.l in the Flow Country, Northern Scotland (Andersen et al., 2018; (Fig. 1a). In1). From the past19th century onwards, management has involved burning to support grouse shooting and artificial drainage of the driest peatlandsareas of peatland, targeted for subsidized agricultural improvement and later afforestation programs (Sloan et al., 2018). More recently, wetter near- -natural areas have been designated for conservation (Lindsay et al., 1988), and previously forestedafforested and drained areas are nowstarted undergoing restoration. Some areas are also actively eroding, particularly at the highest altitudes (Hancock et al., 2018). This complex mosaic of near-natural and modified peatland conditions within this peatlands makes the study site makes it particularly suited to an investigation on the use of InSAR for mapping of peatland condition. To understand the variation and distribution in the characteristics of the APSIS derived time series, we analysed five well-documented 10 to 15 km^2 sub-sites within the study area (Table 1; Fig. 1).

Formatted Table

Formatted: Font: Italic

Formatted: Tab stops: 1.67 cm, Left

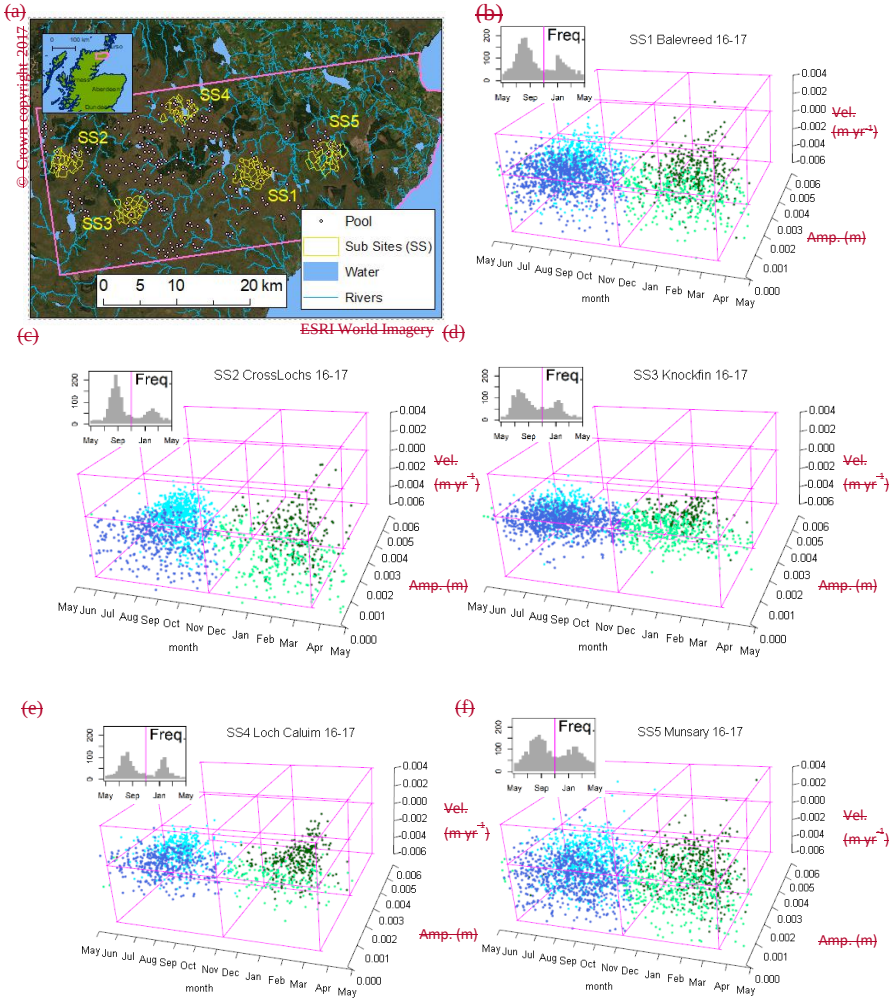

Formatted Table

85

~~Figure 1: Study location, Sub Sites (SS) and the surface motion metrics plots calculated from InSAR detected annual motion~~

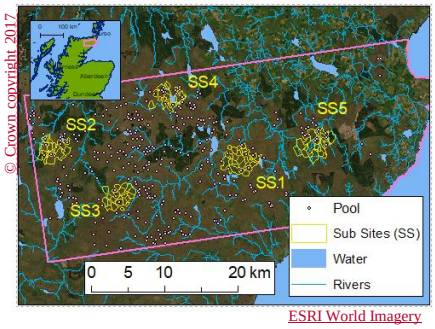

~~between May 10th 2016 to May 9th 2017. (a)~~

Figure 1: The study location (inset) and study area, outlined, in the Flow Country, Northern Scotland. Forested areas are dark green, with the main river network ~~shown. Plots for, (b) SS1 Balavreed, (c) SS2 Cross Lochs, (d) SS3 Knockfin Heights, (e) SS4 Loch Caluim, (f) SS5 Munsary. Axis: x, time (months); y, amplitude (amp.: m), z, velocity (vel.: m yr-1) with inset frequency (Freq.) histograms of peak timing in each of the sub sites. For velocity, +ve is upward and –ve is downward motion of the surface. Histograms of peak timing at all sites display a bimodal distribution and the points on the scatter plots are colored to illustrate their relative position. Pale green and dark blue points are towards the front (low amplitude) and dark green and pale blue points are towards the back (high amplitude). Image sources for (a): ERSI World Imagery, sources Esri~~and location of pool features shown with sub-sites for detailed analysis marked as SS1 to SS5. Credits: ERSI World Imagery, sources ESRI, DigitalGlobe, GeoEye, i-cubed, USDA FSA, USGS, AEX, Getmapping, Aerogrid, IGN, IGP, swisstopo, and the GIS User Community, © Crown copyright 2017. Distributed under the Open Government Licence (OGL). Ordnance Survey (Digimap Licence).

Table 1: Details of the five sub-sites (SS), which are all currently designated as Site of Special Scientific Interest (SSSI), Special Protection Areas (SPA) and Special Areas of Conservation (SAC).

SS	1	2	3	4	5
Name	Balavreed	Cross Lochs	Knockfin	Loch Caluim	Munsary
Location	58.38N	58.39N	58.32N	58.44N	58.39N
	-3.50E	-3.94E	-3.80E	-3.68E	-3.35E
Altitude	~180	~180	~360	~120	~100

Formatted Table

Formatted: Add space between paragraphs of the same style, Don't keep with next

Formatted: Font: Bold

Formatted: Font: Bold

Formatted: Font: Bold

Formatted Table

Formatted: Font: Bold

Formatted: Font: Bold

Formatted: Add space between paragraphs of the same style, Don't keep with next

Formatted: Add space between paragraphs of the same style, Don't keep with next

Formatted: Add space between paragraphs of the same style, Don't keep with next

Formatted Table

(m.a.s.l)					
2					
Topography	**Watershed, gently undulating with pool systems**	**Flat pool systems on watershed with steep slopes into a valley**	**Eroding upland ridge with pools, ephemeral pools, and hags (wind eroded peat islands)**	**Gently sloping basin into central loch**	**Gently undulating area incised by small streams**
General condition	Near-natural	Near-natural, drier peat	Eroding peat	Near-natural	Near-natural including agriculture and forestry
Current management	Low level sheep and deer grazing, conservation management agreement	Low to medium grazing by deer. Includes restoration (forest-to-bog and drain blocking) areas. Conservation management as part of Forsinard Flows National	Deer grazing. Forestry to the north and drainage to the East. Conservation management as part of FFNNR	Low level sheep and deer grazing, under conservation management agreement with FFNNR	Intense drainage for agriculture and grazing surrounded by forestry and forestry to bog to east and South. Part of the site under conservation management by Plantlife Scotland.

		Nature Reserve (FFNNR)			
History	Evidence of damage from historic burning, peat cutting and drainage (hill drains) in places alongside natural drainage lines.	Surrounded by restoration areas (forest-to-bog undertaken in 2006) and standing forestry on deep peat. Wildfire in 1981	The surrounding areas have been drained and burnt in the past.	Some historic drainage and peat cutting. The area was also historically used for cattle grazing and is part of an old drove road.	Historic drain blocked with plastic piling in 2003. Historic drainage and burning.

3 Materials and Methods

23.1 DataInSAR and time series processingpreparation

InSAR surface motion time series were calculated at a pixel resolution of 80 x 90 m across the study site. To calculate the surface motion, we used 410 Sentinel-–1A and –1B synthetic aperture radar images (Descending Orbitdescending orbit 125) gathered every 6 to 12 days between 12/03/March 12th 2015 and 01/06/July 1st 2019 from the European Space Agency Copernicus Open Access Hub (https://scihub.copernicus.eu). Satellite interferometry was applied using these images with the Advanced Pixel System using Intermittent SBAS (APSIS) technique. This technique, which was formerly known as the intermittent small baseline subset (ISBAS), is an advanced DInSAR technique (Sowter et al., 2013). The APSIS technique contains an adapted version of the established SBAS DInSARDifferential InSAR time series algorithm (Bateson et al., 2015; Cigna and Sowter, 2017). It was designed to improve the density and spatial distribution of survey points to return measurements in vegetated areas, where DInSARDifferential InSAR processing algorithms habitually struggle due to incoherence (Osmanoğlu et al., 2016; Gong et al., 2016).

Formatted Table

Formatted: Font color: Text 1, Pattern: Clear

The APSIS algorithm was implemented using Terra Motion Limited's in-house Punnet software, which covers all aspects of processing from the co-registration of SLC (Single Look Complex) data to the generation of time series (~~54). Maximum~~ Sowter et al., 2016). Standard interferometry image thresholds were: maximum horizontal baseline ~~was restricted to~~ no more than 250m ~~with~~, a maximum temporal separation of 1 year between image pairs using a coherence threshold of 0.25, and a minimum multi-look point acceptance threshold of 360~~.~~ to a resolution of 80 by 90 m. Motion was measured relative to a stable reference point, a building on glacial till, at Wick Airport (58.4533° N, 3.0879° W). ~~–~~Phase unwrapping was implemented using an in-house implementation of the Statistical-cost, Network-flow Algorithm for Phase Unwrapping (SNAPHU ~~algorithm (55). Using APSIS, two~~; Chen and Zebker, 2001). Two products were produced for each georeferenced pixel location ~~at approximately 80 by 90 m resolution. A motion~~, the multi-annual average velocity (m yr^{-1}) of the time series ~~of multiannual average~~ calculated from the radar line-of-sight ~~velocity (m yr-1),~~ and the 6 - 12 day time series of surface motion ~~from which we are able to detect~~that detects the seasonal expansion and contraction (or bog breathing) as annual oscillations in relative height (~~L.~~ Alshammari, et al., 2018). Each motion time series was then processed as follows:

~~Each motion time series was processed as follows, to quantify the specific peatland surface motion metrics. Firstly~~First, using the R programming environment (R Core Team, 2013), the time series was sub-sampled into equal time intervals of 12 days, to match the longest overpass interval of Sentinel~~–~~1 images since Sentinel~~–~~1B, which reduces overpass times to 6 days, was not operational until 2016. Outliers were re-estimated using the R 'tsclean' function (Box and Cox, 1964), from R package 'Forecast' (~~R.~~ Hyndman et al., 2020). Gaps were filled with a linear interpolation using the R 'approx' function (Becker et al., 1988) from R 'stats' package (R Core Team, 2020) after 'spline' interpolation methods were found to produce contradictory results ~~when considering~~with adjacent time series across the largest gaps. The 'detrend' R function aligned and reset each time series around zero by subtracting the mean. ~~Secondly,~~

Second, Multichannel Singular Spectrum Analysis (MSSA) using the SSA-MTM toolkit (Ghil et al., 2002; SPECTRA, 2021) was applied to ~~extract~~isolate the cyclical, annual seasonal ~~trend from~~component of the ~~4-year 5-month~~ time series~~. Covariance was calculated~~ from regional climate trends. The MSSA procedure initially calculates covariance after channel reduction with Principal Component Analysis (PCA~~). Using a~~), then using moving ~~window~~windows of 2-12 months, long enough to capture annual cycles, we ~~calculated~~recovered 80% of the signal variance in the first ~~10 PCA channels and~~ 20 Empirical Orthogonal Functions (EOFs~~) to identify~~), which included the seasonal cycles in the time series. In the first instance, surface motion time series were reconstructed using EOFs 1 - 6 ~~(Fig. 2).~~ This reconstruction captured the seasonal cycles but also included longer-term climate trends, notably three wetter years leading to the 2018 European wide drought (Buras et al., 2020). This climate trend causes merging and shouldering of peaks that compromised the detection of the seasonal cycles, particularly in the west of the study area, where it is wetter. To overcome this difficulty, we used a surface motion time series reconstruction using EOFs 5 and 6 (Fig. 2; Supplement 1.1 Fig. S1) which extracted only the seasonal cycles. ~~As the 2018 drought caused severe and widespread subsidence it subdued the multiannual average velocity. This was mitigated by recalculating multiannual~~

Formatted Table

Formatted: Font color: Text 1, Border: : (No border)

Formatted: Font color: Text 1, Border: : (No border)

Formatted: Font color: Text 1, Border: : (No border)

Formatted Table

~~average velocity for three complete motion cycles (March 2015 to March 2018) prior to the 2018 drought.~~ The final MSSA reconstruction provides a signal of relative movement, not absolute surface height (Fig. 2).

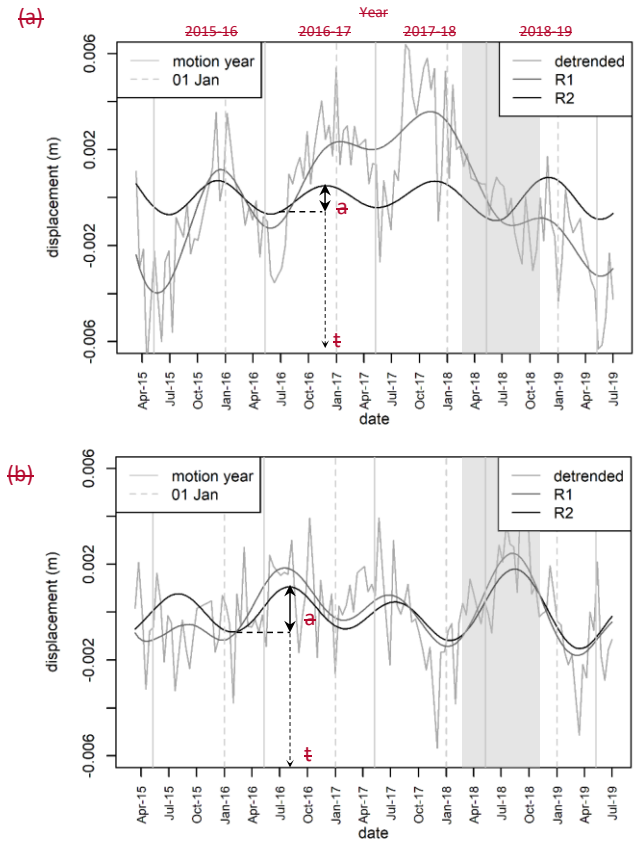

Formatted Table

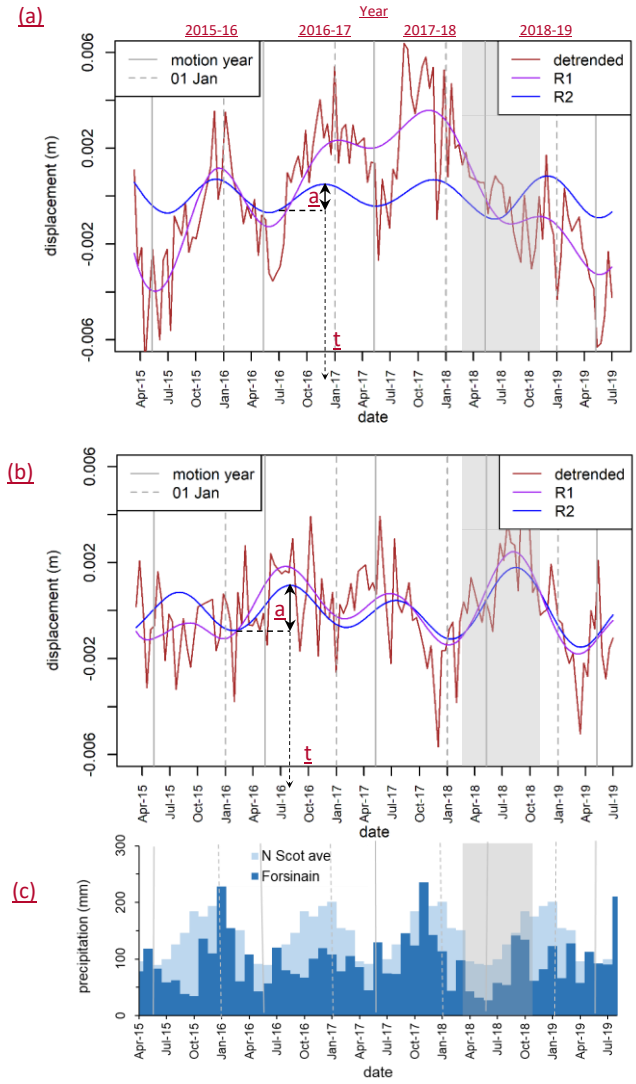

Figure 2: Examples of surface motion time series, and the metric definitions for (a) 'soft' wet bog and (b) a 'stiff' drier bog, calculated from Sentinel-1 APSIS InSAR time series data between ~~12~~ March 12th 2015 and 01 July 1st 2019. against (c) monthly precipitation for northern Scotland (UK Met Office 20 year average, light blue) and Forsinain in the Flow Country (Scottish Environment Protection Agency, Dark blue). The initial mean detrended time series (~~grey~~brown), and Multichannel Singular Spectrum Analysis (MSSA ~~Reconstructions (R)~~ reconstructions, (R1) retaining the local climate trend (~~R1, mid grey~~purple, a combination of empirical orthogonal functions 1 - 6) and R2 annual seasonal cycles (~~R2, dark grey~~blue, a combination of empirical orthogonal functions 5 and 6) are shown. The two surface motion metrics used in the analysis are, peak ~~amplitude~~ timing (dotted line, t), and amplitude (solid line, a) shown for the ~~annual~~ surface motion year May 10th 2016 to May ~~09th~~9th 2017. A third surface motion metric, ~~multiannual~~multi-annual average velocity is not ~~defined~~illustrated here as it is part of the InSAR data processing (~~Materials and Methods~~Sect. 3.1). This asynchronous timing of peaks between (a) and (b) forms a bimodal distribution in the peak amplitude timing of the peatland landscape. The drought event of 2018 ~~is indicated by the shaded column~~ (Buras et al., 2020) is shaded and can be seen to influence ~~the~~relative surface motion with a local climate trend in the 'soft' wet bog (a). ~~For MSSA details see Materials and Methods.~~

~~Peak timing and amplitude of the seasonal cycles~~Third, the MSSA reconstructions were ~~extracted (Fig. 2)~~then analysed for ~~individual years,~~two of three surface motion metrics used to represent the condition of the peatland within each pixel for each motion year using the R 'pracma' peak-find function (R Core Team, 2013). ~~For measurement purposes, the start of the year was set to May 10th to avoid splitting~~Metric one, the ~~period in which~~ date of the ~~seasonal~~annual peak ~~was likely~~'swelling' in the seasonal cycle (peak timing) of the MSSA reconstruction within 12 months from mid-May (Fig. 2). This has been shown to relate to peatland ecohydrology (Alshammari, et al., 2020; Tampuu et al., 2020). Metric two, the annual maximum amplitude (m) in the surface motion signal (amplitude) measured from the previous seasonal minimum of the MSSA reconstruction (Fig. 2). This is an indicator of the elastic response of the peat to changes in water storage (Roulet, 1991; Waddington et al., 2010). ~~be detected. The measurement was not performed on the first and last years in the time series (2014 to 2015 and 2018 to 2019) as surface motion cycles are truncated preventing the accurate calculation of amplitude and peak timing. Surface motion~~ Metric three, is the multi-annual average velocity (m yr^{-1}) of the peatland surface calculated directly and previously described from the APSIS processing. This is a measure of vertical peatland growth (greater positive value) or subsidence (greater negative value) calculated over a fixed section of the time series (Sowter et al., 2013).

As the 2018 drought caused severe and widespread subsidence, it was found to have subdued the multi-annual average velocity and for this reason, we concentrated our analysis between May 10th 2015 and May 9th 2018, discarding the drought period. Multi-annual average velocity was recalculated accordingly. While the impacts of climate anomalies on the time series were ~~also tested~~noticeable and interesting, the first step is to ~~find~~ gain an understanding of how InSAR data can be used to characterise peatland condition, and we focus on this aspect. We also screened time series with multiple peaks per annum or years where ~~detection was~~peaks were not ~~discernable~~discernible, and these pixels were classed as having ~~Irregular~~irregular cycles ~~(IRR).~~ Irregular time series made up 8.4% of the data set and are commonly associated with water courses and damaged bog (including agriculture and some forested ~~areas) (Fig. 4~~pixels). Exclusion of these irregular time series ~~from the surface metrics plot (Fig. 1)~~ does not affect our conclusions. Additionally, for the first and last years in the time series (2014 to 2015 and 2018 to 2019) as many surface motion time series are truncated preventing the accurate calculation of amplitude or peak

Formatted Table

Formatted: Superscript

Formatted: Font color: Text 1, Border: : (No border)

timing in those years the mapping can be incomplete, so for clarity we show most results for 2016 to 2017. To understand the relationships between the three metrics with respect to peatland condition we visualised the metrics in a 3-axis plot.

2.2 Ecohydrology of study area and sub-sites

The Flow Country peatlands exist in a range of topographic, hydrological and management settings, leading to a range of different conditions e.g., from highly eroded to relatively intact peatlands, superimposed by activities such as forestry, drainage, and grazing across an undulating landscape. We predicted that the values of the three motion properties would spatially vary from one place to another showing as small variations on the shape of the 3-axis cluster plot as the values in in amplitude, velocity, and timing subtly shift from place to place. To demonstrate this, the five areas of peatland covering a range of conditions, roughly 10-15 km², defined as the sub-sites, were chosen based on local expert field knowledge and are summarized in Table 1.

Table 1: Details of the five subsites (SS), which are all currently designated as Site of Special Scientific Interest (SSSI), Special Protection Areas (SPA) and Special Areas of Conservation (SAC).

SS	1	2	3	4	5
Name	Balavreed	Cross Lochs	Knockfin	Loch Caluim	Munsary
Location	58.38N -3.50E	58.39N -3.94E	58.32N -3.80E	58.44N -3.68E	58.39N -3.35E
Altitude (m.a.s.l)	≈180	≈180	≈360	≈120	≈100

Formatted Table
Formatted: Add space between paragraphs of the same style, Don't keep with next
Formatted: Font: Bold
Formatted: Font: Bold
Formatted: Font: Bold
Formatted Table
Formatted: Font: Bold
Formatted: Font: Bold
Formatted: Add space between paragraphs of the same style, Don't keep with next
Formatted: Add space between paragraphs of the same style, Don't keep with next
Formatted: Add space between paragraphs of the same style, Don't keep with next

Topography	Watershed, gently undulating with pool systems	Flat pool systems on watershed with steep slopes into a valley	Eroding upland ridge with pools, ephemeral pools, and hags (wind eroded peat islands),	Gently sloping basin into central loch	Gently undulating area incised by small steams
General condition	Near-natural	Near- natural, drier peat	Eroding peat	Near- natural	Near natural surrounded by agricultural conversion and forestry
Current management	Low level sheep and deer grazing, conservation management agreement	Low to medium grazing by deer. Includes restoration (forest-to-bog and drain blocking) areas. Conservation management as part of Forsinard Flows National Nature Reserve (FFNNR)	Deer grazing, Forestry to the north and drainage to the East. Conservation management as part of FFNNR	Low level sheep and deer grazing, under conservation management agreement with FFNNR	Intense drainage for agriculture and grazing surrounded by forestry and forestry to bog to east and South. Part of the site under conservation management by Plantlife Scotland.

Formatted Table

History	Evidence of damage from historic burning and drainage (hill drains) in places alongside natural drainage lines.	Surrounded by restoration areas (forest to bog undertaken in 2006) and standing forestry on deep peat. Wildfire in 1981	The surrounding areas have been drained and burnt in the past	Some historic drainage and peat cutting. The area was also historically used for cattle grazing and is part of an old drove road.	Historic drain blocked with plastic piling, Historic drainage and burning

3.2.3 Ecohydrological classification of the sub-sites

To identify the links between surface motion and the ecohydrology, the The training bed of the sub-sites SS1 to SS5 were divided manually using Google Earth images, into 130 smaller polygons (most between hereafter, sub-site polygons). Polygons ranged from (0.3 –to 0.6 km^2). To construct), a practical size (a) for reliable field and map-based validation and (b) to be appropriate for capturing key features of the landscape (e.g., pool systems, forestry or restoration blocks, streams and banks). To find boundaries between the polygons, one of the authors without specialist peatland knowledge usedsearched for distinct contrasts where there were changes in the landscape structure, e.g. pool systems, visible drainage, vegetation reflectance and, evidence of land use management, e.g. fields and drainage as well as consistency in peak timing. In addition to the sub-site polygons, 125 random points were selected across the whole study area using the ESRI ArcMap "random point" tool. The immediate area close to the point was assessed for features in the landscape, (e.g., topographic setting, natural drainage, evidence of drainage ditches and where these features would influence hydrology, forestsforestry plantation, restoration, land management and the likely range, consistency or inconsistency in peak timing)). This was possible using Google Earth, maps and usedthe InSAR data (Supplement 1.2, Fig. S2). An additional set of 125 polygons were randomly selected across the whole study area using the ESRI ArcMap 'random point' tool (hereafter, random polygons). The immediate area close to drawthe point were similarly assessed for features in the landscape, to define the polygon boundaries to include this variation (most between 0.2 – 0.5 km^2). While the sub-sites included the continuum of conditions and features adjacent to each other, the random polygons captured ensured that there was an improved capture of the ecohydrological statestates across the whole study area and avoided sample bias from, reducing the likelihood that the sub-sites. Measures of topography (average may have excluded a particular ecohydrological state. Summary statistics, of the three surface motion metrics were calculated for each polygon. Average altitude, slope and aspect for all InSAR points in theeach polygon) were also calculated from the Shuttle

Radar Topography Mission Digital Elevation Model (Jarvis et al., 2008) ~~for each polygon (~~to provide measures of topography (Supplement 1.3).

The full set of polygons (sub-sites and random polygons) was then passed to one of the authors with specialist peatland knowledge and based locally for a ~~"blind"~~'blind' (i.e., without prior knowledge of, or information about InSAR metrics~~)~~ within the polygons) ground based eco-hydrological classification. ~~-~~For each polygon, the cover of ~~Plant Functional Types~~plant functional types (PFTs~~);~~; *Sphagnum*, other mosses, shrub, sedges, grasses, rushes, and conifer trees) and the presence of hydrological features (pools, streams, drains, erosion gullies, slope), were recorded using a semi-quantitative scale, (0 = not present or scarce, 1 = present, 2 = co-dominant, 3 = dominant). Current management (conservation, drainage for agriculture and peat cutting, forestry, restoration by forest-to-bog, ~~and~~ restoration by drain blocking, and wind-farm construction) and historical management (e.g., burning, land-use conversion including wind-farm ~~construction,~~development, and restoration), was also documented for each polygon. ~~This was achieved through a combination of existing data, field visits, local knowledge, 1:50 000 UK Ordnance Survey maps, NatureScot National Vegetation Classification maps (64), and Google Earth imagery.~~ The author responsible for classification visited and surveyed all the sub-site polygons and 86 of the random polygons (~~85% of the polygons).~~i.e., 85% of all polygons) by walking across the polygon. For the random polygons where access was not permitted, shared local knowledge from stakeholders (land managers, project officers on the ground, wardens, and gamekeepers) was used instead of a field visit. In all cases, this was complemented with a combination of existing data, 1:50 000 UK Ordnance Survey maps, NatureScot National Vegetation Classification maps (SNH, 2019), and Google Earth imagery. Using the semi quantitative scores, the ~~vegetation~~PFT and hydrology polygon attributes were clustered by similarity using a Hierarchical Cluster Analysis (HCA; Supplement 1.4, Fig. ~~S3) to identify similar combinations of vegetation.~~S3). To avoid an overly split hierarchical tree with only one or two members per cluster requiring complex explanation, it was deemed more informative to ~~analyze~~analyse the ~~vegetation~~PFTs, hydrology and the topography ~~category's~~categories separate from each other. For the ~~vegetation~~PFTs, once the ~~classes had been clustered~~clustering was complete, the average score ~~for~~of the semi-quantitative scale of each ~~category~~PTF in the cluster was ranked ~~with the~~. The top three PFTs were used to characterize and name the plant functional group composition. Absence of a PFT was also noted to assist interpretation (Tables S1-S4). For data visualization of the results, clusters were further grouped based on the dominant PFT, resulting in five plant functional groups: *Sphagnum*, Shrub, Grass, Bare peat (where Low or Absent vegetation was dominant) and Forestry~~. Very few clusters had~~ (Table 2). The four polygons that were dominated by rushes (R) ~~and all those~~ had shrub as a co-dominant vegetation, so they were incorporated into the Shrub group. While ~~sedges~~Sedges (Sg) were co-dominant in ~~both~~many *Sphagnum* and ~~mostly~~ shrub ~~clusters~~polygons, they were not the dominant PFT in any clusters and therefore did not form a separate group. ~~These categories are used and expanded in the captions of Table 2.~~

Table 2: Percentage proportion of clusters derived from Hierarchical Cluster Analysis based on plant functional types (PFTs) represented in the polygons of the five sub-sites and the random polygons. Clusters are defined by the dominant (first) and co-

Formatted Table

Formatted: Font: Italic

Formatted: Font: Italic

Formatted: Font: Italic

dominant (subsequent) PFTs. PFT notations: Sp = *Sphagnum*, S = Shrub, Sg = Sedges, M = Moss, G = Grasses, R= Rushes, F= Forest, LoA = Low or absent vegetation (~~Brash~~brash, bare peat following tree felling or restoration activities etc.). PFT in brackets denotes a notable presence. n=number of polygons. For data visualization, clusters were grouped based on the dominant PFTs in five plant functional groups: Sphagnum, Shrub, Grass, Bare peat and Forestry. Clusters dominated by Rushes (R) were incorporated in the shrub group for data visualization given their low number and shrub co-dominance. ~~The group's~~ Bare peat and Forestry were ~~kept~~retained despite low numbers, as their vegetation is associated to specific management intervention.

Group Name	Sub-~~sites~~site Clusters	SS1	SS2	SS3 %	SS4	SS5	Random Clusters	All %
~~SPH~~Sphagnum	**Sp,S,Sg**	37.9	29.6	0	45.5	19.2	**Sp,Sg,S**	28
~~SHRUB~~Shrub	**S,Sg,Sp(G)**	17.2	14.8	0	13.6	0	**S,Sg,M/ Sp**	28
	S,Sg,R	10.3	48.1	3.8	4.5	34.6	**S,Sg,G,M**	8
	S,Sg,M	20.7	0	69.2	9.1	0	**S,G,R**	8
	S,Sg,M(G)	3.4	0	23.1	18.2	0		
	R,S	0	0	0	0	3.8	**R,Sg,S**	4
~~GRASS~~Grass/ rushes	**G,S,R**	10.3	3.7	0	4.5	11.5	**G,R,S, nSp,nM**	8
	G,R	0	0	0	4.5	11.5	**G,S,R**	1.6
~~BARE~~Bare	**LoA**	0	0	0	0	7.7	**LoA**	4
~~FOR~~Forest	**F**	0	3.7	3.8	0	3.8	**F**	9.6
	***n*=**	*26*	*27*	*26*	*22*	*29*	***n*=**	*125*

We also categorized topography into ~~1 = low, 2 = med~~equal altitude belts, 0-150 m, 151-300 m and ~~3 = high~~301-450 m, and split slope face direction into four quadrants ~~and passed~~(north, east, south and west facing) and ran the ~~data through an~~ HCA. Except for the highest most eroded SS3 site, altitude and aspect did not show any meaningful cluster groups and played no further part in the analysis. The lack of topographic relationships are largely due to the gentle relief of the Flow Country that has few sheltered slopes and deep valleys. Instead, we used average gradient (degrees) in the polygon and found a natural breakpoint at 1.5 degrees that split the dataset equally between ~~FLAT~~Flat (< 1.5 degrees) and ~~SLOPE~~Slope (>1.5 degrees~~), with most pools with).Sphagnum found in FLAT (Fig. 3a).~~

Formatted Table

Formatted: Font: Italic

Formatted: Justified

Formatted: Font: +Body (Times New Roman), Bold, Font color: Text 1

Formatted: Font: +Body (Times New Roman), Bold, Font color: Text 1

Formatted Table

Formatted Table

Formatted: Caption, Line spacing: single

~~(a)~~

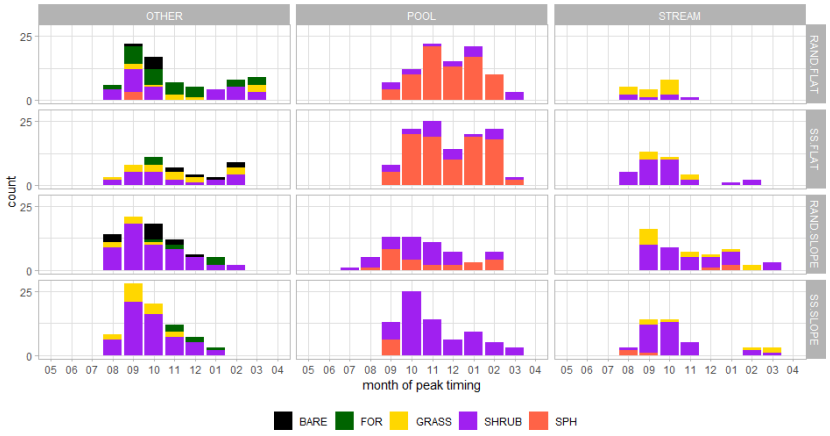

~~(b)~~

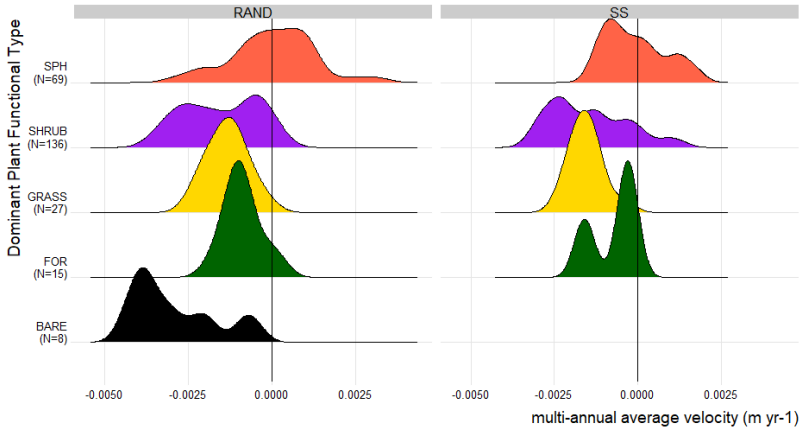

~~(c)~~

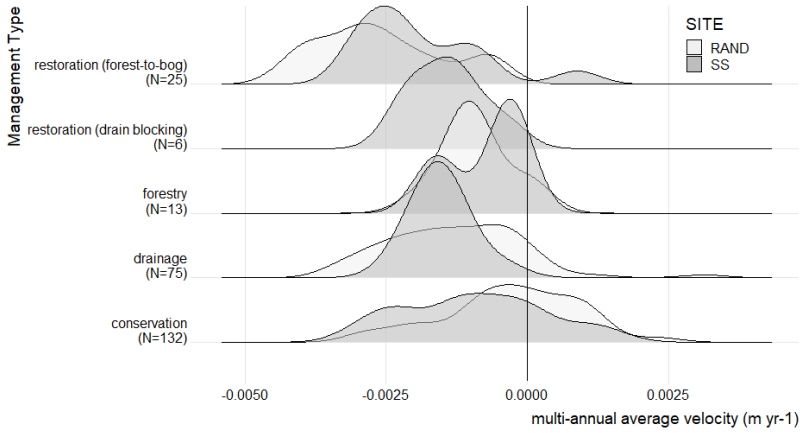

~~(d)~~

3.3

~~**Figure 3: Polygon summaries with respect to dominant plant functional clusters, management groups, topography and the three motion metrics. (a) Distribution of median polygon peak timing over time (month) for dominant plant functional clusters for polygons with pools, streams or other hydrological feature (e.g. drains, erosion gullies, peat cutting, or no apparent features) in either FLAT (gradient < 1.5°) or SLOPE (gradient > 1.5°) topographic setting. Plant functional clusters: BARE = bare peat, FOR = conifer plantation, GRASS = grass-dominated communities, typically Molinia caerulae, SHRUB = shrub dominated communities, typically Calluna vulgaris and/or Erica tetralix, SPH = Sphagnum dominated communities. Sedges, rushes and other mosses are also present, often as co-dominant species in both SPH and SHRUB communities (see Table 2). Months are numbered from May~~**

Formatted Table

Formatted: Line spacing: 1.5 lines

(05) through to the following April (04). (b) Joy plots showing the variation in multiannual velocity for each plant functional group, polygon type (RAND= Random, SS=sub-site) and topography. (c) Joy plots of multiannual average velocity for different management groups (restoration, forestry, drainage, conservation) by polygon type (RAND, SS). (d) The timing of and relative amplitude for three consecutive years (2015-2018) with respect to slope gradient (degrees), dominant plant functional clusters (GRASS, SHRUB and SPH), and by polygon type (RAND, SS).

Summary statistics of the three surface motion metrics were made for each polygon. Although one side of the binomial distribution usually dominated, the median score of each polygon was used over the mean. This is because the transitional nature of the environment (i.e. a wet peat center has drier edges with slightly different vegetation composition), where polygon edges may consist of some pixels from the opposite side of the bimodal distribution (Fig. 1b-f) causing a slight skew in their distributions. The use of the median score was found to reduce these effects for Fig. 3d.

2.4 Mapping the state of the peatland system

To test whether the metrics of peak timing, amplitude and multiannual velocity can be used to map and predict peatland condition we classified the position of pixels within the surface motion metrics Within the 3-axis plot. The classification was based on the Euclidian distance from what restoration practitioners would consider a reference, we then chose a point corresponding to a good condition 'wet' Sphagnum peat. This is characterized by with a winter peak timing, a high amplitude (e.g., 0.008 m), a and extreme positive multiannual velocity (e.g., 0.006 m yr-1), and the most frequent peak timing of the 'wet' Sphagnum dominated condition (e.g., February) within a plot of amplitude vs. peak timing vs. multiannual velocity for the entire study area.velocity, normally associated with 'soft' wet, *Sphagnum* peat and mapped the whole study area relative to that point. The actual reference point was selected by isolating the points that peaked in the winter, then stepping down through the percentiles of the metrics distributions until the case with, the most frequent timing, (e.g., February), highest positive velocity (e.g., 0.006 m yr-1) and highest amplitude (e.g., 0.008 m) was identified. It would also be possible to integrate field observations and choose the reference point values from specific pixel(s) if a particular condition was to be investigated. Data for each pixel wereFor the condition mapping, data for all other points in the 3-axis plot were then paired with thethis reference point and the Euclidian distance between them in 3-dimensional (Cartesian) space was calculated. IfBased on the subsequently observed bimodal distributions (Sect. 4; Fig. 3), if the paired pixelpoint was in the 'dry' shrubopposite side of the bimodal distribution to the reference point, the Euclidian distance was mapped as a 'V' shaped path via zero velocity and zero amplitude at the mid date, 10th November, between the 'wet' Sphagnum and 'dry' shrub conditions.earlier and later timed clusters in the distribution. Prior to calculation, the positions of the outer portions of the 'wet' and 'dry' distributions 3-axis plot were adjusted. This is because if the paired point is earlier thanbefore (left of) the dryearlier peak and later thanafter (right of) the wetlater peak the difference between the peak timing and the origin would be incorrectly estimated.overestimated. To mitigate this, these cases were folded inwards along the axis of the peak of their distributions (effectively turning the upturned 'W' shape of the bimodal distribution into an 'M' shape). Using the natural breaks (Jenks) classification as a guide in ESRI ArcGIS as a guide, thresholds were used to map 'wet' Sphagnum dominated, 'dry' shrub dominated and the thin/modified peat

Formatted Table

Formatted: Superscript

~~classes across the whole study site~~classify distance from the 'soft' wet Sphagnum point. These values were then mapped to produce an ecohydrological ~~map (Fig. 4d).~~classification across the whole study site.

~~To verify the predictive accuracy of the~~ To further validate our ecohydrological classification map, we remotely identified and marked the central locations of all the pool systems ~~(328 in total),~~ within the study area (328 in total) using Google Earth images~~,~~ and ~~compared~~determined if these ~~points~~markers corresponded to the ~~Sphagnum 'wet' condition. To capture the wider~~'soft' wet Sphagnum state. Although 'soft' wet areas in which *Sphagnum* is dominant do not necessarily contain pool systems, pool systems in this area almost always contain 'soft' wet peat. Furthermore, in the study area, pool systems provide a spatially distributed, abundant and easily identifiable sample of this part of the peatland system. They also correspond to the part of peatland systems most unequivocally associated with 'near-natural' ecohydrological condition in this type of upland blanket bog. As the position of each pool marker did not take into account that pool systems often display complex morphology, varying geometries (and sometimes variable condition) ~~of a full pool system (~~related to local hydrological conditions (Goode, 1973; Lindsay, 2016~~), a search~~) there was a need to tolerate a level of spatial uncertainty. To capture this, a wider area of 150m (using the buffer function in ESRI ArcMap) was ~~then~~ calculated~~.~~ around the marker. This buffer area contained at least 3 by 3 pixels of the ecohydrological map. We ~~than~~then calculated the percentage of ~~Sphagnum 'wet' pixels~~pixels identified in the ecohydrological classification as 'soft' in the buffer. Pixels classed as irregular were not included in the count (Table S5).

Formatted Table

Formatted Table

(a)

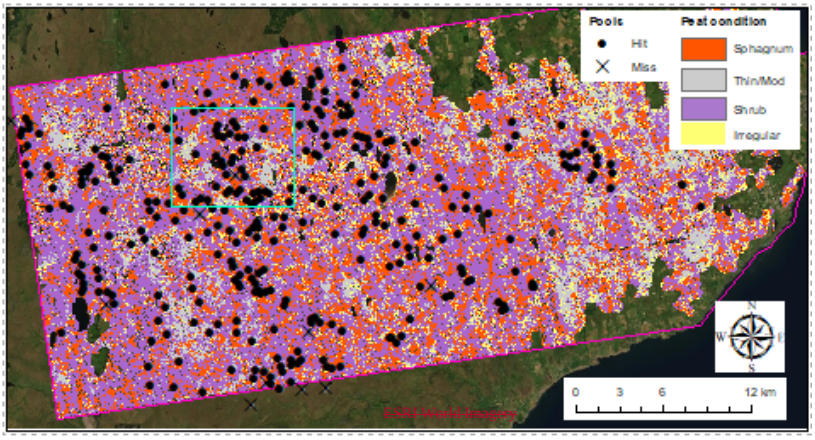

(b)

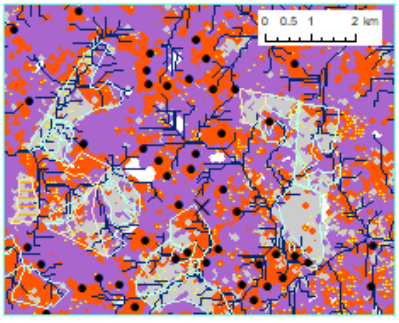

(c)

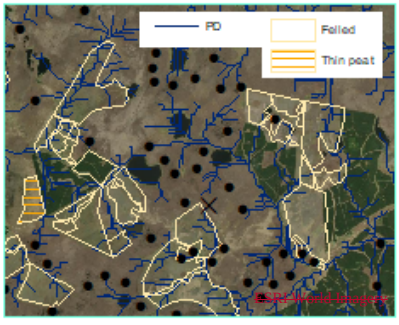

(d)

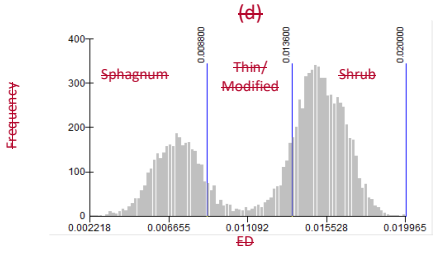

Formatted Table

Figure 4: The classification of peatland condition, with respect to the location of pool systems, and areas of forest-to-bog restoration in the study area. (a) Classified map based We acknowledge that we focus **on the Euclidian distance (in 3-dimensional Cartesian space) from the position of a 'wet' Sphagnum endmember of each point in the plot of peak timing, amplitude and multiannual velocity for the period June 2016 to May 2017. Three peat classifications are indicated, Sphagnum, Thin/modified, and Shrub. Pixels that could not be classified due to an absence of distinct seasonal oscillation are classified as irregular. The classified area (approx. 930 km^2) was delineated using peat soils from the National Soil Map of Scotland (JHI, 2021). Points in pool systems that have been correctly classified are shown as a "hit" and those incorrectly classified as a "miss". (b) A detailed view of the classified area highlighted within (a) illustrating the relationship with potential drainage (PD), determined from a DEM, areas of thin peat (hatched), and peat areas at various stages of forest to bog restoration (outlined) ranging from recently felled (thin/modified class) to almost fully restored via rewetting (Sphagnum class). (c) A true colour satellite image of area, (b). Some of these restoration areas now have** one particular state of peat, which does not account for the presence of drier, thin or damaged peat **conditions of wet peat. (d) Frequency distribution of Euclidian distance, and the thresholds used to highlight the three peat conditions, Sphagnum dominated, Thin/modified and Shrub dominated. Images sourced via ESRI ArcMap in 2021. The variability seen within the felled forest blocks reflects variable degree of recovery associated with varying starting conditions, time since initiation of restoration (ranging from 0 to >15 years), landscape position and technique of the intervention. Image source for (a) and (c) ESRI World Imagery: Esri, DigitalGlobe, GeoEye, i-cubed, USDA FSA, USGS, AEX, Getmapping, Aerogrid, IGN, IGP, swisstopo, and the GIS User Community.**

3 Results

3.1 Surface motion in blanket peatland

InSAR surface motion time series and long-term average motion were generated for the period March 12th 2015 to July 1st 2019. In the timeseries, the height of the surface was calculated relative to its first point and was determined every 6 days at pixel resolution 90 x 80 m. Indeed, stiffer, thin and damaged peat cannot readily be associated with a single, well-defined and remotely identifiable feature distributed across the whole study site. Seasonal cycles, subsiding during the summer and rising in the winter were observed in time series from the majority of pixels. From this, we defined a motion year beginning at the least active period in May and thus avoided dissection of the peaks in the distribution. We then focused our analysis area in the same way. For instance, whilst drains can be observed from Google Earth, their age, maintenance and the extent of their impact on the period May 10th 2015 to May 9th 2018 to minimize uncertainties from a drought in mid to late 2018 (Buras et al., 2020), and illustrate data for the central year, 2016 to 2017, where the buildup and continuation of adjacent years is complete. peat would require further evidence beyond the scope of this study.

Multichannel Singular Spectrum Analysis (MSSA) was applied to the dataset to isolate this cyclical, annual seasonal component of the time series (Fig. 2) and the following three surface motion metrics used to represent the condition of the peatland within each pixel. Metric one, the timing (date) of the annual peak in the seasonal cycle within 12 months from mid-May (4 Results

From the frequency histograms of Fig. 2). This has been shown to relate to peatland ecohydrology (L. Alshammari, et al., 2020; Tampuu et al., 2020). Metric two, the annual maximum amplitude (m) in surface motion measured from the previous seasonal minimum (Fig. 2). This is an indicator of the elastic response of the peat to changes in water storage (Roulet, 1991; Waddington et al., 2010). Metric three, the multiannual average vertical velocity (m yr-1) of the peatland surface. This is a

Formatted: Font color: Text 1, Border: : (No border)

measure of peatland growth (positive value) or subsidence (negative value) calculated over a fixed section of the time series (Sowter et al., 2013; Materials and Methods).

To understand the variation and distribution of our metrics across a spectrum of peatland conditionspeak timing, we plotted them over five well-documented 10 to 15 km^2 sub-sites within the study area. These sub-sites span a range of landscape settings and ecohydrological conditions, from a gently undulating low-lying watershed with well-developed pool systems to actively eroding high plateau (Table 1, Fig. 1a). Plots of the metrics from the sub-sites all show features ofdiscovered a bimodal data distribution with respect to annual peak timing (Fig. 1b-f).distribution, showing an early and late peak (Fig. 3a), and defined the motion year to begin at the least active swelling period on May 10th to avoid dividing periods of maximum swelling into consecutive calendar years. The bimodal distribution peaks fall between August to October and December to February. Each sub-site shows a variation in the range of amplitude and velocity (Fig. 1b-f),, similarly illustrated in the 3-axis plots (Fig. 3b-f). For each of the sub-sites, the plots of the three motion metrics show small variations on the shape and position of the data cluster reflecting the diversity of peatland conditions sampled across the landscape.

Formatted Table

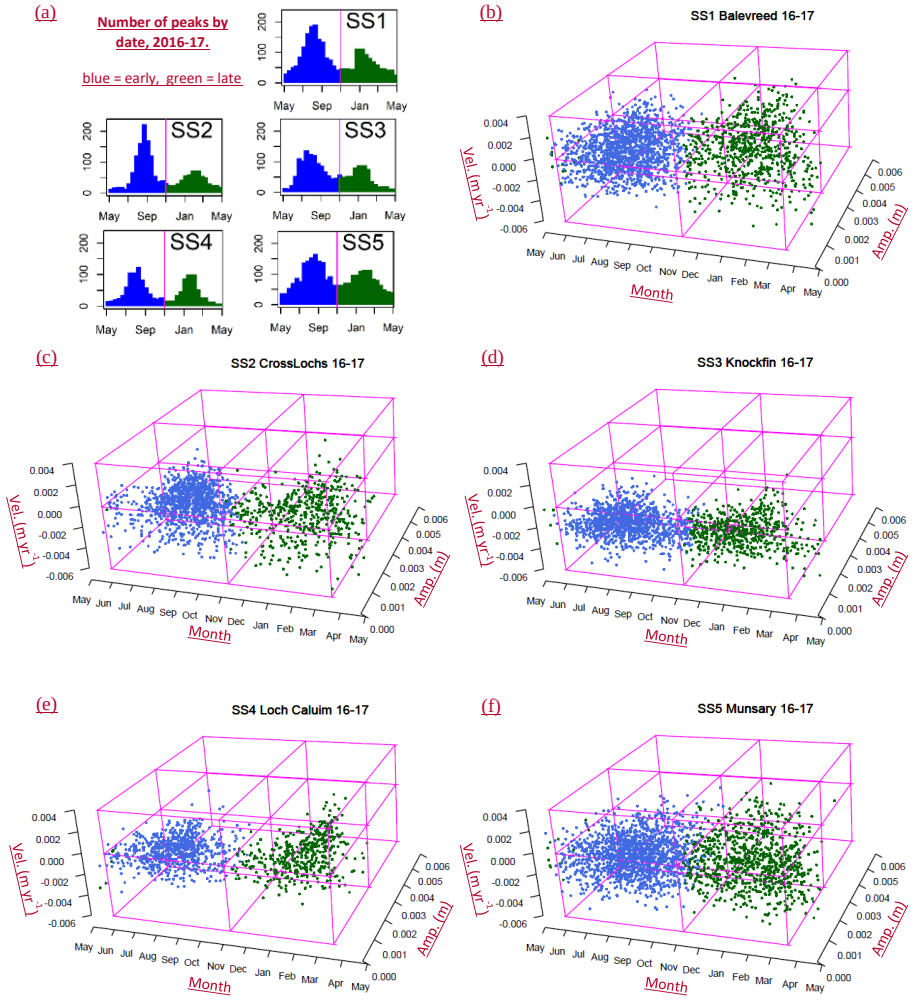

Figure 3: 3Characteristics of the motion metrics by Sub-Site (SS) calculated from MSSA reconstructions of the InSAR detected annual motion between May 10th 2016 to May 9th 2017. (a) Frequency of peak timing throughout the motion year where May is the

Formatted Table

Formatted: Line spacing: 1.5 lines

period of least surface motion activity, with a binomial distribution split at 10th November into an early (blue) and late (green) cluster. (b to f) 3-axis plots of the surface motion metrics, (b) SS1 Balavreed, (c) SS2 Cross Lochs, (d) SS3 Knockfin Heights, (e) SS4 Loch Caluim, (f) SS5 Munsary. Axis: x, peak time (Month); y, amplitude (Amp.: m), z, multi-annual average velocity (Vel.: m yr^{-1}). For multi-annual average velocity, greater +ve is peatland growth and greater –ve is peatland subsidence. Magenta box is for visual reference. Each sub-site demonstrates a specific range in peatland condition according to the plot space they occupy.

4.2 Relationship between surface motion and eco-hydrology

~~To understand the link between the surface motion metrics and peatland condition, we divided the sub-sites into 130 polygons (0.2 to 0.6 km^2) in which metrics were aggregated. Additionally, 125 similarly sized individual polygons were generated, randomly distributed across the whole study area. This size was practical for reliable field and map-based validation and meaningful for capturing key features of the landscape (e.g., pool systems, forestry or restoration block, stream and banks). Dominant plant functional types (Sphagnum, sedges, shrub, grass, bare peat, forestry), hydrological features (pools, erosion gullies, streams, drainage ditches), topographic setting (slope, elevation) was recorded for each polygon and used for eco-hydrological classification (Materials and Methods; SI Appendix).~~

~~A hierarchical clustering approach (~~The HCA~~; Fig. S3)~~ revealed ecological groups relating to dominant plant functional types that were comparable between the sub-~~sites~~site and random polygons (Table 2) as well as hydrological groups separating polygons with pool systems and ~~those~~polygons with streams from all other polygons~~. Comparison of~~ (Fig. S3). When the HCA ~~based~~ classifications and topographic information (slope) were compared to the surface motion metrics ~~enables~~, we determined the following consistent relationships ~~to be determined~~ for the sub-~~sites~~site and random ~~sites, as follows. First, shifts~~site polygons:

4.2.1 Timing, hydrology and topography

Shifts in the ~~polygon monthly~~ peak timing distributions relate to a combination of topography, hydrology, and plant functional group (Fig. ~~3a).~~4), and peak timings themselves were consistent within groups between the three motion years. *Sphagnum*-dominated polygons are almost exclusively associated with Pools and more so on Flat ground with a tendency to have a peak later in the year than the most other hydrological and topographical combinations of vegetation or hydrological features. Within the hydrological class ~~POOL~~Pool, polygons with topographic gradients greater than 1.5°~~(RAND SLOPE, SS SLOPE),~~° (Slope) for both random and subsite polygons, have their highest ~~monthly~~peak timing frequencies earlier in September and ~~or~~ October than polygons ~~on flatter ground~~ with topographic gradients less than 1.5°~~(FLAT~~° (Flat), which tend to ~~be~~peak in November, January and February. The steeper gradients, ~~RAND SLOPE, SS SLOPE~~in both random and sub-sites, tend to be associated with ~~SHRUB~~shrubs and ~~GRASS~~ grass-dominated vegetation ~~types~~communities with low frequencies of *Sphagnum* dominated polygons ~~(SPH).~~ Polygons with ~~POOL~~pools as the dominant hydrological feature tend to have their highest frequencies from October onwards, later than polygons ~~with STREAM or OTHER, independent of being FLAT or SLOPE. Sphagnum-dominated polygons (SPH) are almost exclusively associated with POOLS and flat ground (RAND FLAT, SS FLAT), and~~

Formatted Table

Formatted: Font: Italic

~~tend to have their highest monthly frequencies later in the year (November to February) than the other hydrological and topographical situations which are mainly SHRUB dominated polygons as well as the other PFTs, such as GRASS, FOR and BARE.~~classed as stream or polygons with other features (drainage ditches, peat cutting or erosion gullies).

~~Second,~~

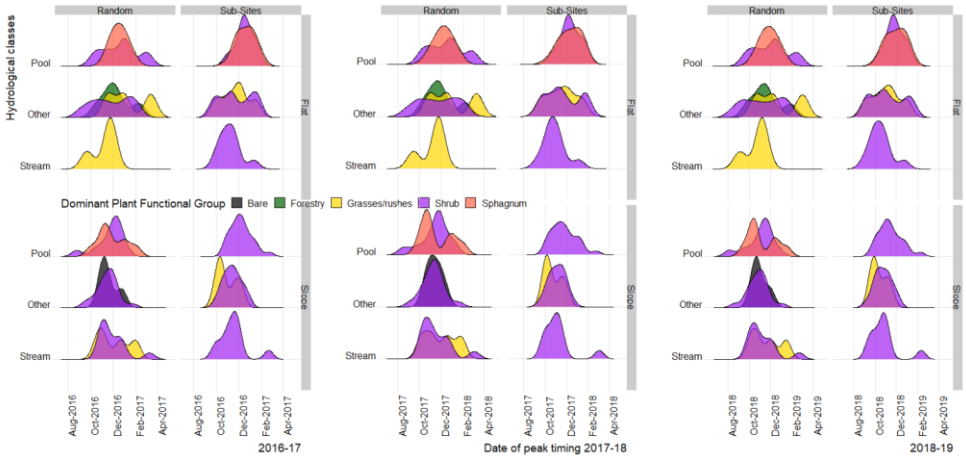

Figure 4: Distribution of mean peak timing date by dominant plant functional clusters for polygons with Pools, Streams or Other hydrological features (e.g., drains, erosion gullies, peat cutting, or no apparent features) in either a Flat (gradient < 1.5°) or Slope (gradient > 1.5°) topographic setting for the ~~most positive values of multiannual~~Random and Sub-site polygons. Plant functional group polygons (*n* random/subsite): Bare = bare peat (6/2), Forestry = conifer plantation (12/3), Grasses/rushes = grass-dominated communities (13/14), typically *Molinia caerulae*, Shrub = shrub dominated communities (59/77), typically *Calluna vulgaris* and/or *Erica tetralix*, Sphagnum = *Sphagnum* dominated communities 35/34. Sedges, rushes and other mosses are also present, often as co-dominant species in both *Sphagnum* and Shrub communities (see Table 2).

4.2.2 Multi-annual average velocity and dominant plant functional group

Multi-annual average velocities that were most positive (gain of mass over time) were almost entirely dominated by *Sphagnum* (~~SPH, Fig. 3b~~5). Polygons with plant functional ~~types~~groups typically associated with natural or man-made drainage (~~SHRUB~~Shrub), disturbance (forestry ~~(FOR)~~ and bare peat ~~(BARE~~) or thin, degraded peat (~~GRASS~~Grasses) consistently displayed negative long-term ~~(multiannual)~~multi-annual average velocities (loss of mass over time) regardless of topographical setting. Sites in which ~~grass~~grasses or ~~forestry~~forest dominate tend to have a more intermediate ~~multiannual~~multi-annual average velocity than either ~~SHRUB~~Shrub or *Sphagnum* ~~(SPH)~~ dominant polygons. Where bare peat is dominant, ~~the~~ multi-annual average velocities are lowest (most negative ~~velocities occur.~~).

~~Third, when multiannual~~

Formatted Table

Formatted: Font: Italic

Formatted: Font: Italic

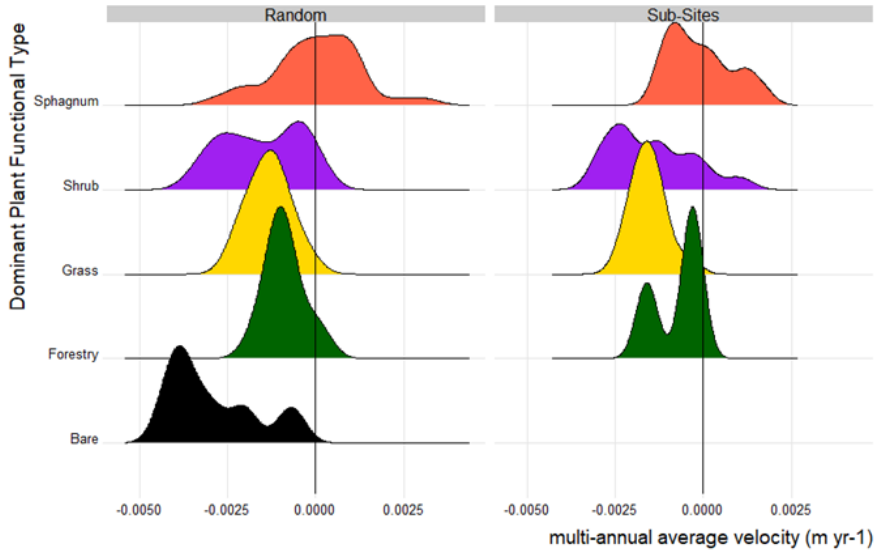

Figure 5: Distribution density of multi-annual velocity for each plant functional group and polygon type Plant functional polygons *n* (random/subsite): Bare = bare peat (6/2), Forestry = conifer plantation (12/3), Grasses/rushes = grass-dominated communities (13/14), typically *Molinia caerulae*, Shrub = shrub dominated communities (59/77), typically *Calluna vulgaris* and/or *Erica tetralix*, Sphagnum = Sphagnum dominated communities 35/34. Sedges, rushes and other mosses are also present, often as co-dominant species in both Sphagnum and Shrub communities (see Table 2).

4.2.3 Multi-annual average velocity and management

When multi-annual average velocities are compared across different management classes (Fig. ~~3c~~6), the least negative values are observed under conservation management and most negative values are associated with forest-to-bog management, a restoration approach that typically involves compaction from heavy machinery during the removal of conifer stands, followed by drain blocking and surface re-profiling. This restoration class shows a broader distribution in long term ~~multiannual~~multi-annual average velocity than other management classes, reflecting variable degree of recovery associated with differing starting condition, time since initiation (ranging from 0 to >15 years) and techniques used in the intervention.

Formatted Table

Formatted Table

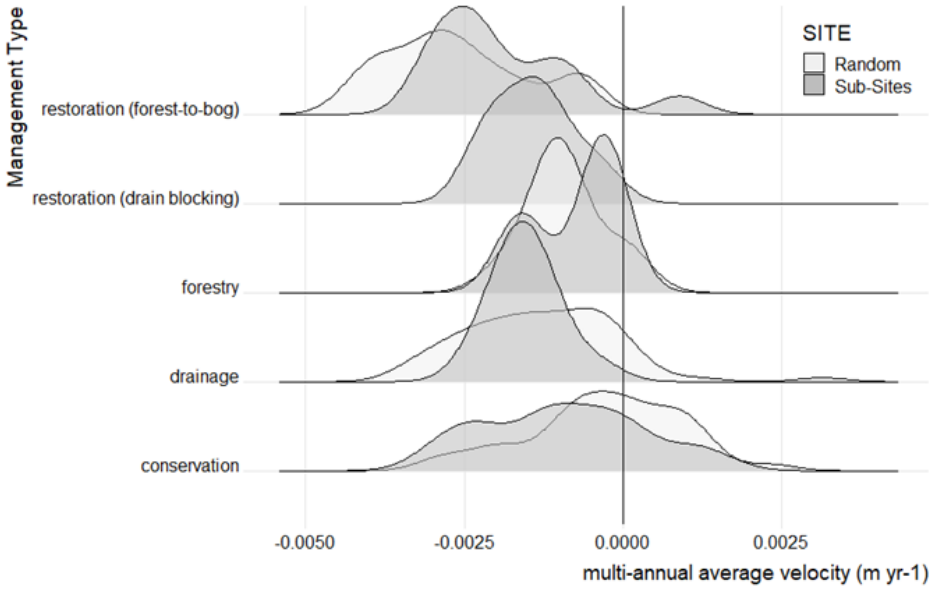

Figure 6: Distribution density of multi-annual average velocity for different management groups and by polygon type (Sub-site and random). Management polygons *n* (Random/Sub-Site): restoration (forest-to-bog) 12/13, restoration (drain blocking) 0/6, forestry 10/3, drainage 62/13, conservation 37/95.

4.2.4 Time and magnitude of peatland swelling

The factors ~~controlling~~that influence amplitude can be deduced from relative annual amplitude change and peak timing plots for the three most dominant PFT clusters (~~SHRUB, SPH~~Sphagnum, Shrub and ~~GRASS~~Grass) across three surface motion years (Fig. ~~3d~~7). These graphs all show a ~~strong linear relationship~~positive trend between timing (day of year) and amplitude with a tendency for higher amplitudes usually occurring later in each surface motion year. Steeper slopes ~~are more likely~~tend to have the lower amplitudes that peak earlier in ~~each~~the surface motion year. ~~Shallower~~Shallow to flat slopes ~~are more likely~~tend to have higher amplitudes and peak later in the surface motion year. ~~There is also year~~ Year-on-year variation in range of observed amplitudes is apparent, with a large range in 2015-2016 and smaller ranges in the two subsequent years. We attribute this to inter-annual variation and antecedent conditions in rainfall (e.g., Fig. ~~seasonal~~ 2c). A relatively dry 2014-2015 resulted in a strong amplitude~~, likely to~~ response in 2015-2016 with lesser responses in the two subsequent wetter years. These differences can be related to ~~interannual variation in the local water table coupled with~~ the amount of ~~available~~ unfilled pore

space in the uppermost layer of the peat. ~~In this sequence the polygon sites indicate that the peatland became gradually~~In essence, as the peat gets wetter and the pore space fills, there is less capacity in the peat to add more water and the amplitude response diminishes. A more saturated~~, to the point that by 2017-2018 there were relatively fewer pores to fill, and annual surface motion was reduced.~~

~~Synthesizing the above, the bimodal distribution of peatland surface motion timing within our landscape may be interpreted as reflecting two dominant components of the landscape, a drier shrub dominated and a wetter Sphagnum dominated component. Wetter, flatter sites in a 'near natural condition', typically dominated by SPH PFT tend to reach peak surface heights later in the year, have higher amplitudes and stable-positive velocities. Drier SHRUB and GRASS PFT dominated sites tend to reach peak surface heights earlier in the year, have lower amplitude oscillations and negative velocities. That the distribution of surface motion metrics in this particular blanket bog landscape is bimodal reflects a combination of the natural~~ state of the peatland ~~and the legacy of past management.~~in 2016-2017 and 2017-2018 was also noted in field observations.

~~3~~

Figure 7: Timing of and relative amplitude for three consecutive years (2015-2018) with respect to slope gradient (degrees), dominant plant functional type (PFT; Grass, Shrub and *Sphagnum*), and by polygon type (Sub-site and random).

4.3 Application to large area condition mapping

The observed relationship between surface motion metrics and ecohydrology is readily interpreted in the context of reported field measurements of peat surface motion (Howie and Hebda, 2018; Morton and Heinemeyer, 2019). Flatter sites under near natural conditions are poorly drained, wetter and dominated by *Sphagnum* spp. In turn, *Sphagnum* spp. have a considerable capacity for water storage as a direct result of their physiology (Kellner and Halldin, 2002), resulting in peak water storage and seasonal swelling of the surface ~~late~~later in the year. Drier sites with compacted peat have less capacity to store water and reach water holding capacity earlier in the autumn (Price, 2003). Furthermore, the more degraded peat in these sites is less elastic and therefore exhibits a lower amplitude response to changes in water storage (Holden et al., 2004; Lui and Lennartz, 2019). As the seasonal water balance shifts, drier, better drained sites lose water first followed by the *Sphagnum* sites which may continue to swell on account of a hysteresis during the first stages of water loss (Howie and Hebda, 2018). Synthesizing Sect 4.2 (Fig. 4-7) the bimodal distribution of peatland surface motion timing within our landscape may be interpreted as reflecting two dominant components of the landscape. Wetter, flatter sites, typically dominated by *Sphagnum* and sedges are 'soft' peats, they tend to reach peak surface heights later in the year (December to February window), have higher amplitudes and more positive velocities. Drier shrub and grass dominated sites are 'stiff' peats, they tend to reach peak surface heights earlier in the year (August to October window), with slightly (but not exclusively) lower amplitude oscillations and more negative velocities. Additionally, in the 3-axis plot there are points characterized by both low amplitudes, negative velocities, and peak timings that can also fall outside the window of the 'soft' and 'stiff' class. These subtle variations of the metrics identified a third broad ecohydrological class which reflects thin peats, the most degraded and drained grass dominated sites or sites under restoration that are in transition to either a 'soft' or 'stiff' state.

~~With this interpretation of the relationship between the surface motion metrics and ecohydrology, it should be possible to use the InSAR time series to map peatland condition. To illustrate this approach and evaluate its potential, a classified condition map was generated (Fig. 4a). This map was based on the classified Euclidian distance (Materials and Methods) from an ideal 'wet' Sphagnum-dominated reference point (positive velocity, high amplitude, late winter peak timing) within a plot of amplitude vs. peak timing vs. multiannual velocity for the entire study area. The resulting histogram of Euclidian distance (Materials and Methods) was split into three broad peatland classes (Fig. 4). A Sphagnum class characterized by winter (December to February) peak timing, high amplitude, and stable to positive velocity). A shrub class characterized by distinct autumn (August to October) peak timing with lower amplitude and negative velocities. A thin/modified peat class, characterized by both low amplitudes, negative velocities, and peak timing dissimilar to either the 'Sphagnum' or 'shrub' class. These thin/modified areas are expected to correspond with the most degraded and drained grass dominated sites or sites under restoration that are in transition to either a Sphagnum or shrub dominated state.~~

Formatted Table

Formatted: Font: Italic

Formatted: Font: Italic

Formatted: Font: Italic

~~To assess the predictive accuracy of the Sphagnum class we determined the proportion of 328 pool systems that coincided with pixels of that class. Although wet areas in which Sphagnum is dominant do not necessarily contain pool systems, the reverse is nearly always true, and in the study area pool systems provide a spatially distributed, abundant and easily identifiable sample of this part of the peatland system. They also correspond to the part of peatland systems most unequivocally associated with 'near-natural' ecohydrological condition. The shrub and thin/modified classes are more likely to correspond with areas in between on sloping, degraded, forested and formerly forested peatland, some of which may have been much wetter prior to drainage.~~

~~A single marker was positioned in each selected pool system and the accuracy of the method determined based on whether this marker lies within 150 m of a correctly classified pixel. There is a need to tolerate a level of uncertainty as pool systems often display complex geometry related to local hydrology (Goode, 1973; Lindsay, 2016) and the position of the marker point could not take this into account. On this basis, identification of wet peat conditions around the pool systems is 97.9% accurate. Detailed inspection of the remaining 2.1% (7/328) of pool systems~~Mapping and applying thresholds to the Euclidian distance calculations into these three broad peatland classes relative to the 'soft' peat condition generated the peatland condition map (Fig. 8a). The classification produced patchwork of conditions in the Flow Country and the map evidences the widespread occurrence of the 'stiff' peat condition associated with both naturally drier areas on the slopes and wet 'soft' peat margins but also areas made drier by land use history of burning and drainage. The impact of restoration activities, following the felling of forestry on deep peat in the last 25 years can also be seen: recent forest-to-bog clearance is displayed as 'thin/modified' peat whilst areas well on their way to recovery are showing as either the 'soft' or 'stiff' condition (Fig. 8b-c). In polygons where forest is planted on peat, the signal is much more mixed with a greater proportion of the irregular class. This mixture is a result of the poorer SAR response over trees and the variable conditions encountered within forest stands. For example, in these forestry plantations, fire breaks, gaps between blocks (termed 'rides') and riparian areas that were never planted can still be wet, 'soft' and *Sphagnum* rich in contrast with the planted blocks themselves. Furthermore, plantations may enclose areas of deep peat with pools, and may display variable wetness and dryness depending on site and topography.

Formatted Table

Formatted Table

(a)

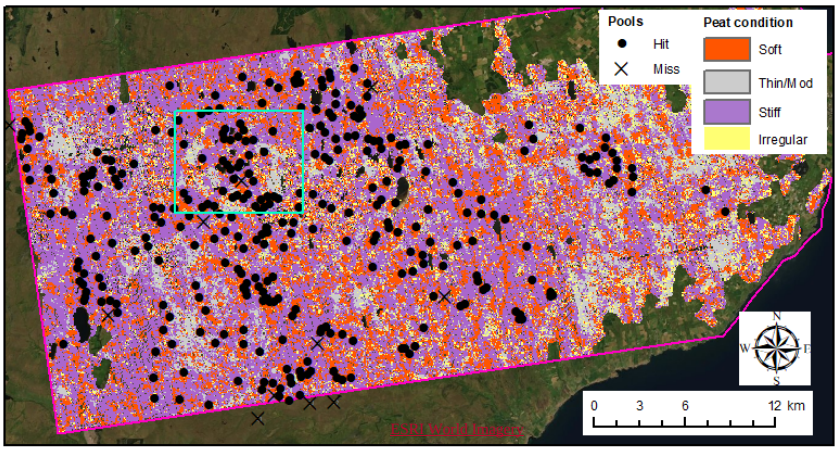

(b)

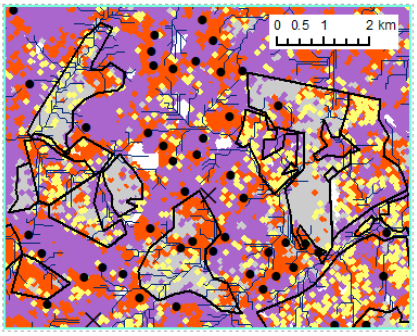

(c)

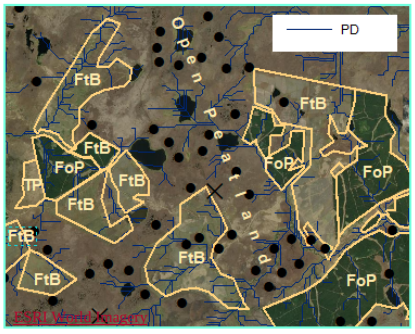

(d)

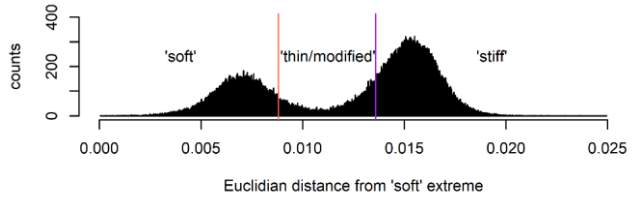

Formatted Table

Figure 8: The ecohydrological classification of 'soft', 'thin/modified', and 'stiff' peatland condition, with respect to the location of pool systems, and areas of forest-to-bog restoration in the study area. (a) Classified map based on the Euclidian distance (in 3-dimensional Cartesian space) from the position of the 'soft' reference to all other points in the 3-axis plot of peak timing, amplitude and multi-annual average velocity, including the screened irregular time series for the period June 2016 to May 2017. Pool systems that have been correctly classified are shown as a 'hit' otherwise as a 'miss'. (b) A detailed view of the classified area highlighted within (a) illustrating the relationship with hydrology, determined from a DEM (potential drainage, PD) and polygons delineating areas for restoration. (c) A true colour satellite image of area showing the restoration status of the polygons, un-felled forest on peat (FoP), peat areas at various stages or different years of forest to bog (FtB) restoration and an area of thin peat (TP) (d) Frequency distribution of Euclidian distance, and the thresholds used to differentiate the three peat conditions. Credits: The classified area (approx. 930 km^2) was delineated using peat soils from the National Soil Map of Scotland (JHI, 2021). Images sourced via ESRI ArcMap in 2021. Image source for (a) and (c) ESRI World Imagery: Esri, DigitalGlobe, GeoEye, i-cubed, USDA FSA, USGS, AEX, Getmapping, Aerogrid, IGN, IGP, swisstopo, and the GIS User Community.

Using the criteria for the remote validation that pool systems should always fall in the 'soft' peat category, 97.9 % of the pool system markers were identified to have occurred within 150 m of that class. Detailed inspection of the remaining 2.1% (7/328) of pool system markers that did not fall within our threshold reveals that these pool systems all showed evidence of localized erosion or drainage causing degradation of their natural hydrology. ~~From this, we can deduce that our method is converging towards 100% accuracy~~While not validated in ~~identifying Sphagnum dominated pool systems in a near natural ecohydrological condition.~~

~~Inspection~~the same way, further inspection of our classification ~~relative to other known features~~combined with specialist knowledge of the area indicates that the thin/modified class corresponds to areas under restoration, notably areas recently felled for forest ~~to~~ bog restoration, areas subject to intensive grazing, thin peat soils on steeper higher ground and in valley bottoms (e.g., Fig. ~~4b,~~8b-c). The abundance of the 'thin/ ~~modified~~modified' class is striking in the east of the study area and we note that this corresponds to long-term historical usage of the land for agriculture and associated cutting of peat for fuel (Andersen et al., 2018; Minasny et al., 2019).

~~Our~~Within the area, our method identifies approximately 254 km^2 (27.3 % of the area) as 'soft' wet *Sphagnum* dominated peat, 481 km^2 (51.7 %) as 'stiff' shrub dominated peat, 117 km^2 (12.8 %) as the 'thin/modified' peat class with 78 km^2 (8.4 %) as irregular time series. This classification ~~also~~therefore provides an overall measure of the current state of this blanket bog landscape, to which future regional change, on account of climate change or restoration, may be compared. ~~For example, within the area, our method identifies approximately 254 km^2 (27.3 % of the area) as wet Sphagnum dominated peat, 481 km^2 (51.7 %) as shrub dominated peat, 117 km^2 (12.8 %) as the thin/modified peat class with 78 km^2 (8.4 %) as irregular time series.~~

~~4~~

5 Discussion

Our most important finding is that surface motion metrics derived from APSIS InSAR time series enable almost continuous spatial and temporal characterization of peatland condition at large scales. That the SAR data can penetrate cloud cover, measures regular physical displacement of the surface, and captures a known dynamic ~~behavior~~behaviour associated with peat resilience gives this approach a significant lead over the far more challenging effort to measure peatland condition from optical reflectance data~~. This is compounded by the fact that cool wet peatlands are often obscured by cloud (Minasny et al., 2019).~~ (e.g. Artz et al., 2019). This is compounded by the fact that peatland areas are often obscured by cloud (Minasny et al., 2019). A valuable exercise would be to quantify the similarities and contrasts of motion mapped peatland condition to optical products and we anticipate that motion data will bring different and complementary information. This may be advantageous for restoration monitoring and information on peatland mechanical condition from surface motion may be key to resolving weaknesses in optical studies, for example in carbon accounting (Couwenberg et al., 2011).

The sensitivity and dynamic response of surface motion metrics to changes in the state of the peatland system should make the method ideally suited to monitoring and informing peatland management and restoration. Globally, large areas of northern ~~peatland~~peatlands degraded by historic drainage, grazing and forestry are now under or targeted for restoration (Rochefort et al., 2017). ~~As a consequence~~Consequently, peatland conservation and restoration are increasingly perceived as critical tools in the fight against global climate change (Leifeld and Menichetti, 2018; Amelung et al., 2020; Günther et al., 2020). Restoration strategies typically involve raising water levels to re-establish wet conditions. The expectation is that this will promote *Sphagnum* establishment, often a key measure of the success of an intervention (Rochefort et al., 2017; Bellamy et al., 2012; Caporn et al., 2018; González and Rochefort, 2019).

In the case of blanket bog landscapes, our finding of naturally 'stiff' drier shrub and 'soft' wetter *Sphagnum* states raises the question as to whether a ~~linear~~ strategy of increasing ~~peat wetness~~*Sphagnum* cover is always an appropriate restoration target, or indeed if it is the only desirable outcome ~~in all peatland settings.~~for blanket bogs. In this context, an APSIS InSAR-based assessment of the condition of a whole ~~peatland~~blanket bog landscape can help guide restoration strategies by~~, firstly~~ first identifying the typical natural states and hydrological structure of that ~~peatland, and secondly~~landscape. Second, following intervention, this approach could enable a robust monitoring of restoration trajectories and outcomes~~.~~ (Marshall et al., 2020). Our study also suggests that when monitoring restoration trajectories over time, the impacts of interannual variabilities such as precipitation on the metrics would likely need to be accounted for.

In natural landscapes, these peatland states are a consequence of landscape evolution in which the vertical accumulation of peat must be counterbalanced on an appropriate spatial and temporal scale by erosion (Large et al., 2021). Drier states correspond to areas of net carbon loss due to natural drainage, incision and erosion along peatland margins, and wetter states correspond to peatland interiors, areas with low gradient, that tend towards carbon accumulation. In this context, to restore a site that is naturally 'stiff' and dry to the 'soft' wet state would risk instability, while the opposite would fail to optimize carbon storage. A more suitable and sustainable ambition is to accept that restored blanket bog sites may follow different trajectories

Formatted Table

Formatted: Highlight

Formatted: Font: Italic

Formatted: Font: Italic

Formatted: Font: Times New Roman, Highlight

towards naturally *Sphagnum* or shrub states, (or 'soft' and 'stiff'), and that these target end states will be constrained by the hydrological landscape setting, as conceptualized by Winter (Winter, 1988). Our approach provides evidence for these natural states co-existing within the study areas, and evidence to guide and monitor appropriate restoration trajectories within this system. Recognizing and preserving this mosaic is critical in maintaining large- and small-scale peatland landscape stability and carbon balances, particularly as long-term models suggest that the natural drying out of peatland is accelerating due to drainage (Harris et al., 2020; Leifeld et al., 2019) and climate change (Gallego-Sala and Prentice, 2013).

The approach outlined here should be readily transferable to alternative peatland settings within different parts of the global peatland climate space. Using surface motion metrics identified from the InSAR time series of peatland motion, a surface deformation space for a given peatland system can be defined. The position of ecohydrological characteristics within this space can then be deployed to quantify the state of the peatland system and map changes with respect to climate change and management intervention. This capacity to customize the approach is valuable as it provides the means to measure peatland condition at a global scale. If realized, this would enhance our understanding of the large-scale functionality of peatland landscapes and provide the robust evidence base required for sustainable peatland management.

Data availability

doi: 10.17639/nott.7123

Supplement Link

Supplement supplied

Author Contribution

A.S. led the processing of the InSAR data that A.V.B. post-processed, analyzed and visualized. R.A. recorded the polygon attributes, mapped the pools, contributed to data visualization and completed the ground surveys with C.M. D.J.L developed the overall idea of applying InSAR for this purpose. All authors were responsible for critical contributions, passing the final manuscript and editing text and figures.

Competing Interests

Andrew Sowter is affiliated with Terra Motion Limited. The APSIS (Advanced Pixel System using Intermittent SBAS) method is owned by the University of Nottingham and is the subject of a UK Patent Application (No. 1709525.8) with the inventor named as Dr. Andrew Sowter; it is currently Patent Pending.

Formatted Table

Formatted: Font: Italic

Formatted Table

Disclaimer

We are not responsible for the consequences of any decisions or actions even if they have been influenced by the material and ideas in this manuscript.

Acknowledgments

The authors would like to thank members of the following organizations who provided access to sites for surveys or insight and local knowledge about past and present management over the study area: NatureScot Peatland ACTION, Royal Society for the Protection of Birds, Plantlife Scotland, Forestry and Land Scotland, Scottish Forestry, Welbeck Estate and Shurrery Estate. David Gee and Ahmed Athab for their assistance with the APSIS InSAR data output. "National Soil Map of Scotland" copyright and database right The James Hutton Institute v.1_4. Used with the permission of the James Hutton Institute. All rights reserved. Any public sector information contained in these data is licensed under the Open Government License v.2.0. R.A. and C.M are funded by a Leverhulme Leadership Award (1466NS) and D.J.L, R.A. and C.M. with a NERC InSAR TOPS NE/P014100/1.

References

Alshammari L., Large D.J., Boyd, D.S., Sowter S., Anderson R., Andersen R., and Marsh S.: Long-term peatland condition assessment via surface motion monitoring using the ISBAS DInSAR technique over the Flow Country, Scotland. Remote Sens., 10, 1-24, doi:10.3390/rs10071103, 2018.

Alshammari, L., Boyd, D.S., Sowter, A., Marshall, C., Andersen, R., Gilbert, P., Marsh, S., and Large, D.J.: Use of surface motion characteristics determined by InSAR to assess peatland condition, J. Geo. Res: Biogeosciences, 125, e2018JG004953, doi:10.1029/2018JG004953, 2020.

Andersen, R., Cowie, N., Payne, R.J., and Subke, J.A.: The Flow Country peatlands of Scotland. Mires and Peat, 23, 1-2, doi:10.19189/MaP.2018.OMB.381, 2018.

Almendinger, J.C., Almendinger, J.E., and Glaser, P.H.: Topographic fluctuations in across a spring fen and raised bog in the Lost River Peatland, northern Minnesota. J. Ecol., 74, 393-401, doi:10.2307/2260263, 1986.

Amelung, W., Bossio, D., de Vries, W., Kögel-Knabner, I., Lehmann, J., Amundson, R., Bol, R., Collins, C., Lal, R., Leifeld, J. and Minasny, B.: Towards a global-scale soil climate mitigation strategy, Nat. Comms., 11(1), 1-10, doi:10.1038/s41467-020-18887-7, 2020.

Artz, R.R.E.; Johnson, S.; Bruneau, P.; Britton, A.J.; Mitchell, R.J.; Ross, L.; Donaldson-Selby, G.; Donnelly, D.; Aitkenhead, M.J.; Gimona, A.; Poggio, L.: The potential for modelling peatland habitat condition in Scotland using long-term MODIS data., Sci. Tot. Env, 660, 429-442, 2019.

Baden, W., and Eggelsmann, R.: Der Wasserkreislauf eines nordwestdeutschen Hochmoores. Verleg Wasser und Boden, Hamburg, Germany, 1964.

Bateson, L., Cigna, F., Boon, D. and Sowter, A.: The application of the Intermittent SBAS (ISBAS) InSAR method to the South Wales Coalfield, UK. Int. J. App. Earth Obs. Geoinform., 34, 249–257, doi:10.1016/j.jag.2014.08.018, 2015.

Becker, R. A., Chambers, J. M., and Wilks, A. R.: The New S Language. Wadsworth & Brooks/Cole, 1988.

Bellamy, P.E., Stephen, L., Maclean, I.S., and Grant, M.C.: Response of blanket bog vegetation to drain-blocking. Appl. Veg. Sci., 15(1), pp.129-135, doi:10.1111/j.1654-109X.2011.01151.x, 2012.

Box, G.E.P. and Cox, D.R.: An Analysis of Transformations. J. R. Stat. Soc. B Methodol., 26(2) 211-252 (1964).

Buras, A., Rammig, A., and Zang, C.S.: Quantifying impacts of the 2018 drought on European ecosystems in comparison to 2003. Biogeosciences, 17(6), 1655-1672, doi:10.5194/bg-17-1655-2020, 2020.

Caporn, S.J.M., Rosenburgh, A.E., Keightley, A.T., Hinde, S.L., Riggs, J.L., Buckler, M. and Wright, N.A.: Sphagnum restoration on degraded blanket and raised bogs in the UK using micropropagated source material: a review of progress. Mires and Peat, 20, 1-17, doi:10.19189/MaP.2017.OMB.306, 2018.

Chen, C.W., and Zebker, H.A.: Two-dimensional phase unwrapping with use of statistical models for cost functions in nonlinear optimization. J. Opt. Soc. Am. A, 18, 338–351, doi:10.1364/JOSAA.18.000338, 2001.

Cigna, F., and Sowter, A.: The relationship between intermittent coherence and precision of ISBAS InSAR ground motion velocities: ERS-1/2 case studies in the UK. Remote Sens. Environ., 202, 177–198, doi:10.1016/j.rse.2017.05.016, 2017.

Crump J. (Ed.), Smoke on water: Countering global threats from peatland loss and degradation. UNEP, GRIDA, GPI, 2017.

S.Fiaschi, E.P. Holohan, M. Sheehy, M. Floris, PS-InSAR Analysis of Sentinel-1 Data for Detecting Ground Motion in Temperate Oceanic Climate Zones: A Case Study in the Republic of Ireland. Remote Sens., 11(3), doi:10.3390/rs11030348, 2019.

Couwenberg, J., Thiele, A., Tanneberger, F., Augustin, J., Bärisch, S., Dubovik, D., Liashchynskaya, N., Michaelis, D., Minke, M., Skuratovich, A., and Joosten, H.: Assessing greenhouse gas emissions from peatlands using vegetation as a proxy. Hydrobiologia volume 674, 67–89, https://doi.org/10.1007/s10750-011-0729-x, 2011.

Fritz, C., Campbell, D.I., and Schipper, L.A.: Oscillating peat surface levels in a restiad peatland, New Zealand – magnitude and spatiotemporal variability. Hydrol. Processes. 22, 3264-3274 doi: 10.1002/hyp.6912, 2008.

Glaser P.H., Chanton J.P., Morin P., Rosenberry D.O., Siegel D.I., Ruud O., Chasar L.I., and Reeve A.S.: Surface deformations as indicators of deep ebullition fluxes in a large northern peatland. Global Biogeochem. Cycles 18, GB1003, doi:10.1029/2002GB002069, 2004.

Gallego-Sala, A.V., and Prentice, I.C.: Blanket peat biome endangered by climate change. Nat. Clim. Change. 3(2), 152-155, doi:10.1038/nclimate1672, 2013.

Formatted Table

Formatted: German (Germany)

Ghil M., Allen M. R., Dettinger M. D., Ide K., Kondrashov D., Mann M. E., Robertson A. W., Saunders A., Tian Y., Varadi F., and Yiou P.: Advanced spectral methods for climatic time series. Rev. Geophys. 40, 1-40, doi:10.1029/2000RG000092, 2002.

Gong, W., Thiele, A., Hinz, S., Meyer, F.J., Hooper, and A., Agram, P.S.: Comparison of small baseline interferometric SAR processors for estimating ground deformation. Remote Sens. 8, 330, doi:10.3390/rs8040330, 2016.

González, E., and Rochefort, L.: Declaring success in Sphagnum peatland restoration: Identifying outcomes from readily measurable vegetation descriptors. Mires and Peat. 24(19), 1-16, doi:10.19189/MaP.2017.OMB.305, 2019.

Goode, D.A.: The significance of physical hydrology in the morphological classification of mires. Classification of Peat and Peatlands. In Proc Int. Peat Soc. Symp., Eds. International Peat Society, Glasgow. pp10–20, 1973.

Günther, A., Barthelmes, A., Huth, V., Joosten, H., Jurasinski, G., Koebsch, F. and Couwenberg, J.: Prompt rewetting of drained peatlands reduces climate warming despite methane emissions, Nat. Comms., 11(1), 1-5, doi:10.1038/s41467-020-15499-z, 2020.

Hancock, M.H., England, B., and Cowie, N.R.: Knockfin Heights: a high-altitude Flow Country peatland showing extensive erosion of uncertain origin. Mires & Peat. 23, 1-20, doi:10.19189/MaP.2018.OMB.334, 2018.

Harris, L.I., Roulet, N.T., and Moore, T.R.: Drainage reduces the resilience of a boreal peatland. Environ. Res. Commun. 2(6), p.065001, doi:10.1088/2515-7620/ab9895, 2020.

Holden, J., Chapman, P.J., and Labadz, J.C., Artificial drainage of peatlands: hydrological and hydrochemical process and wetland restoration. Prog. Phys. Geogr. 28, 95–123, doi:10.1191/0309133304pp403ra, 2004.

Howie, S.A., and Hebda, R.J.: Bog surface oscillation (mire breathing) a useful measure in raised bog restoration. Hydrol. Process., doi: 10.1002/hyp.11622, 2018.

Hutchinson, J. N.: The record of peat wasteage in the East Anglian fenlands at Holme Post, 1848-1978 A.D. J. Ecol., 68, 229-249, 1980.

Hyndman, R., Athanasopoulos, G., Bergmeir, C., Caceres, G., Chhay, L., O'Hara-Wild, M., Petropoulos, F., Razbash, S., Wang, E. and Yasmeen, F.: Forecast: Forecasting functions for time series and linear models. R package version 8.5. URL:http://pkg.robjhyndman.com/forecast, 2019.

Jarvis, A., Reuter, H.I., Nelson, A., and Guevara, E.: Hole-filled seamless SRTM data V4, International Centre for Tropical Agriculture (CIAT), available at http://srtm.csi.cgiar.org, 2008.

JHI, The James Hutton Institute, "National Soil Map of Scotland" available at https://www.hutton.ac.uk/learning/natural-resource-datasets/soilshutton/soils-maps-scotland. Last accessed ~~01 June~~22 Nov. 2021.

Kellner, E., and Halldin, S.: Water budget and surface-layer water storage in a Sphagnum bog in central Sweden. Hydrol. Process., 16(1), 87-103, doi:10.1002/hyp.286, 2002.

Kennedy, G.W., and Price, J.S.: A conceptual model of volume-change controls in the hydrology of cutover peats. J. Hydrol., 302, 13-25, doi:10.1016/j.hydrol.2004.06.024, 2005.

Formatted Table

Kulczynski, S., Peat bogs of Polsie. Memoires de l'Academie Polenaise des Sciences et des Lettres. Class de Sciences Mathematiques et Naturelles. Serie B: Sciences Naturelles. 15, 1949.

Kurimo, H.: Surface fluctuation in three virgin pine mires in eastern Finland. Silva Fennica, 17, 45-64, 1983.

Large, D.J., Marshall, C., Jochmann, M., Jensen, M., Spiro, B.F. and Olaussen, S.: Time, Hydrologic Landscape, and the Long-Term Storage of Peatland Carbon in Sedimentary Basins. J. Geo. Res.: Earth. Surf., 126(3) doi:10.1002/essoar.10503762.1, 2021.

Lees, K.J., Quaife, T., Artz, R.E.E., Khomik, M., and Clark, J.M.: Potential for using remote sensing to estimate carbon fluxes across Northern peatlands: a review. Sci. Tot. Env., 615, 857874, doi:10.1016/j.scitotenv.2017.09.103, 2018.

Lees, K.J.; Artz, R.R.E.; Khomik, M.; Clark, J.; Ritson, J.; Hancock, M.; Cowei, N.; Quaife, T.:Using spectral indices to estimate water content and GPP in sphagnum moss and other peatland vegetation., IEEE Trans. Geo. and Rem. Sen., 58, 4547-4557, 2020.

Leifeld, J., and Menichetti, L.: The underappreciated potential of peatlands in global climate change mitigation strategies. Nat. Commun., 9(1), 1-7, doi:10.1038/s41467-018-03406-6, 2018.

Leifeld, J., Wüst-Galley, C., and Page, S.: Intact and managed peatland soils as a source and sink of GHGs from 1850 to 2100. Nat. Clim. Change., 9(12), 945-947, doi:10.1038/s41558-019-0615-5, 2019.

Liu, H., and Lennartz, B.: Hydraulic properties of peat soils along a bulk density gradient—A meta study. Hydrol. Process., 33(1), 101-114, doi:10.1002/hyp.13314, 2019.

Lindsay, R., Charman, D.J., Everingham, F., O'reilly, R.M., Palmer, M.A., Rowell, T.A. and Stroud, D.A.: The flow country: the peatlands of Caithness and Sutherland. D.A. Ratcliffe and P.H. Oswald Eds. (Nature Conservancy Council, Peterborough 1988), pp174. Available from Joint Nature Conservation Committee (JNCC) via http://jncc.defra.gov.uk/page-4281, 1988.

Lindsay, R.: Peatland Classification. In: Everard, M., Finlayson, C.M., Irvine, K., McInnes, R.J., Middleton, B.A., Davidson, N.C. (Eds.) The Wetland Book: I: Structure and Function, Management, and Methods. Springer Nature, Netherlands, pp.1–14., 2018.

Mahdiyasa, A.W., Large, D.J., Muljadi, B.P., Icardi, M., and Triantafyllou, S.: MPeat—A fully coupled mechanical-ecohydrological model of peatland development. Ecohydro., e2361. https://doi.org/10.1002/eco.2361 2021

Marshall, C., Bradley, A.V., Andersen, R. and Large, D.J.: Using peatland surface motion (bog breathing) to monitor Peatland Action sites. NatureScot Research Report 1269. https://www.nature.scot/doc/naturescot-research-report-1269-using-peatland-surface-motion-bog-breathing-monitor-peatland-action, 2021.

Minasny, B., Berglund, Ö., Connolly, J., Hedley, C., Vries, F. D., Gimona, A., Kempen, B., Kidd, D., Lilja, H., Malone, B., McBratney, A., Roudier, P., O'Rourke, S., Rudiyanto, Padarian, J., Poggio, L., Caten, A. T., Thompson, D., Tuve, C., and Widyatmanti, W.: Digital mapping of peatlands–A critical review. Earth Sci. Rev., 196, 102870, doi:10.1016/j.earscirev.2019.05.014, 2019.

Formatted Table

Formatted: French (France)

Formatted: Font color: Auto

Money, R.P., and Wheeler, B. D.: Some critical questions concerning the restorability of damaged raised bogs. Appl. Veg. Sci., 2(1), 107–116, doi:10.2307/1478887, 1999.

Morton, P.A., and Heinemeyer, A.: Bog breathing: the extent of peat shrinkage and expansion on blanket bogs in relation to water table, heather management and dominant vegetation and its implications for carbon stock assessments. Wetl. Ecol. and Manag., 27, 467–482 doi.org/10.1007/s11273-019-09672-5, 2019.

Mustonen, S.E., and Seuna, P.: Metsaojitusksen vaikutuksesta suon hydrologiaan. Pages 1-63 in Publication 2, National Board of Waters, Finland, Water Research Institute, 1971.

Osmanoğlu, B., Sunar, F., Wdowinski, S., and Cabral-Cano, E.: Time series analysis of InSAR data: methods and trends. ISPRS J. Photogramm. Remote Sens., 115, 90–102, doi:10.1016/j.isprsjprs.2015.10.003, 2016.

Poggio, L., and Gimona, A.: National scale 3D modelling of soil organic carbon stocks with uncertainty propagation—an example from Scotland. Geoderma, 232, 284-299, doi:10.1016/j.geoderma.2014.05.004, 2014.

Price, J.S.: Role and character of seasonal peat soil deformation on the hydrology of undisturbed cutover peatlands. Water Resour. Res., 39(9) 1214, doi:10.1029/2002WR001302, 2003.

Price, J.S., and Schlotzhauer, S.M.: Importance of shrinkage and compression in determining water storage changes in peat: the case of a mined peatland. Hydrol. Process., 13 2591-2601, doi:10.1002/(SICI)1099-1085(199911)13:16<2591::AID-HYP933>3.0.CO;2-E, 1999.

R Core Team, R: A language and environment for statistical computing. R Foundation for Statistical Computing, Vienna, Austria. Available at http://www.R-project.org/, 2013.

R Core Team: 'Stats v3.6.2' R package, available at https://www.rdocumentation.org/packages/stats, 2020.

Reeve, A.S., Glaser, P.H., and Rosenberry, D.O.: Seasonal changes in peatland surface elevation recorded at GPS stations in the Red Lake Peatlands, northern Minnesota, USA. J. Geophy. Res.: Biogeosci., 118, 1616-1626, doi:10.1002/2013JG002404, 2013.

Rochefort, L., and Andersen, R.: Global Peatland Restoration after 30 years: where are we in this mossy world?. Rest Ecol., 25(2), 269-270, doi:10.1111/rec.12417, 2017.

Roulet, N.T., Surface level and water table fluctuations in a subarctic fen, Arc. Alp. Res., 23 (3), 303-310, 1991.

Sloan, T.J., Payne, R.J., Anderson, A.R., Bain, C., Chapman, S., Cowie, N., Gilbert, P., Lindsay, R., Mauquoy, D., Newton, A.J. and Andersen, R.: Peatland afforestation in the UK and consequences for carbon storage, Mires and Peat, 23, doi.org10.19189/MaP.2017.OMB.315, 2018.

SNH, available at http://gateway.snh.gov.uk/natural-spaces/index.jsp (last accessed 24/07/20), 2019.

Sowter, A., Che Amat, M., Cigna, F., Marsh, S., Athab, A., and Almshammari, L.: Mexico City land subsidence in 2014-2015 with Sentinel-1 IW TOPS: Results using the Intermittent SBAS (ISBAS) technique. Int. J. App. Earth Obs. Geo., 52, 230-242, doi:10.1016/j.jag.2016.06.015, 2016.

Formatted Table

Sowter, A., Bateson, L., Strange, P., Ambrose, K., and Syafiudin, M.F.: DInSAR estimation of land motion using intermittent coherence with application to the South Derbyshire and Leicestershire coalfields. Rem. Sens. Lett., 4(10), 979-987, doi:10.1080/2150704X.2013.823673, 2013.

SPECTRA software: http://research.atmos.ucla.edu/tcd/ssa/guide/guide4.html, last accessed 2 May 2021

Tampuu, T., Praks, J., Uiboupin, R., and Kull, A.: Long Term Interferometric Temporal Coherence and DInSAR Phase in Northern Peatlands. Rem. Sens., 12(10), 1566, doi: 10.3390/rs12101566, 2020.

Waddington, J.M., Morris, P.J., Kettridge, N., Granath, G., Thompson, D.K. and Moore, P.A.: Hydrological feedbacks in northern peatlands. Ecohydrol., doi:10.1002/eco.14938(1), 113-127, 2015.

Waddington, J.M., Kellner, E., Strack, M., and Price, J.S.: Differential peat formation, compressibility, and water storage between peatland microforms: Implications for ecosystem function and development. Wat. Res. Res. 46, W07538, doi:10.1029/2009WR008802, 2010.

Winter, T.C.: A conceptual framework for assessing cumulative impacts on the hydrology of nontidal wetlands. Env. Man., 12(5), 605-620, doi:10.1007/BF01867539,1988.

Formatted Table